FLOATING BLADE INSTALLATION

ANALYSING THE DYNAMIC INTERACTION BETWEEN TOWER AND INSTALLATION TOOL

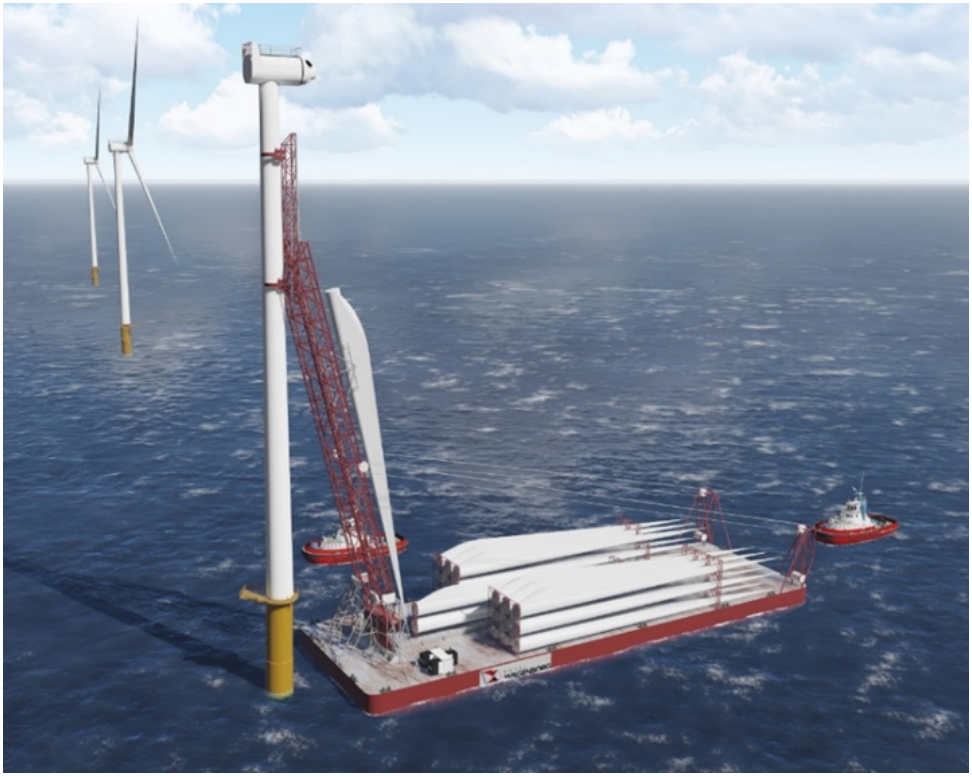

Hil Fon Tang
1504959

Confidential

FLOATING BLADE INSTALLATION

ANALYSING THE DYNAMIC INTERACTION BETWEEN TOWER AND INSTALLATION TOOL

to obtain the degree of Master of Science in 'Offshore and Dredging Engineering'
at Delft University of Technology,

By

Hil Fon TANG

Student number:	1504959	
Project duration:	2 October, 2017 – 29 August, 2018	
Thesis committee:	Prof. dr. A. Metrikine,	TU Delft, Chairman
	Ir. C. Keijdener,	TU Delft, daily supervisor
	Dr. ir. K.N. van Dalen,	TU Delft
	Ir. J. Jacobs,	TWD BV
	Ir. C. Charalambous,	TWD BV

CONTENTS

SUMMARY

The demand for blade installation and maintenance is increasing with each additional installed offshore wind turbine. In 2017, 560 additional turbines were installed in Europe, reaching 4149 turbines in total. Currently, they are serviced with cost and time inefficient methods, such as rope access and jack-up vessels. Rope access is slow and requires the deployment of expensive technicians in dangerous environments. Jack-up vessels are overqualified, expensive and not readily available. Identifying the short comings of these methods, TWD saw an opportunity to design a dedicated tool for blade installation. This resulted in the floating Blade Installation Tool (BIT).

The BIT is a state-of-the-art solution that allows for blade installation from a floating platform. By incorporating motion compensation and decoupling it can mitigate the vessel motions, thereby reducing the relative motion of the top element of the BIT. After the BIT is connected to the tower, a blade handling kart can safely transport and install the blades to and from the nacelle.

The goal of this thesis is to gain insight in the dynamic behaviour of the system, with the focus on the interaction between the turbine and the BIT. For this purpose, a numerical model is created for the governing plane of motions, the vertical plane on the longitudinal axis of the vessel. Using this model, several simulations are performed under a variety of conditions to assess the BIT for the following sub-questions:

- Are the interface forces on the tower acceptable in conditions comparable to the operational limits of jack-up vessels?
- What is the relation between the vessel-tower distance and the interface forces?
- How much does the significant wave height affect the forces and stresses on the tower?

The results show that the BIT's motion compensation system will effectively mitigate the first order wave force induced motions of the vessel. However, it also shows that at multiple stages of the lifting process the BIT will exert a force exceeding the allowable force limits. To satisfy the constraints imposed by the tower manufacturers, adaptations to the design of the BIT must be made.

Some of the possible solutions to be explored are as follows: The increase in contact surface area between the BIT and tower. The stresses, which is the limiting factor, are reduced allowing for higher interface forces. Applying additional mechanical systems, such as winches and hydraulic cylinders, to add an additional layer of control to the system. This is expected to be a necessary option, although it will increase the complexity of the tool.

1

INTRODUCTION

I seem to have been only like a boy playing on the seashore, and diverting myself in now and then finding a smoother pebble or a prettier shell than ordinary, whilst the great ocean of truth lay all undiscovered before me.

Isaac Newton

The first chapter presents the introduction to the thesis subject, the floating blade installation tool. First, it discusses briefly the background information and the reasons supporting the development of a new blade installation tool. Next, a brief overview of the tool and its components are presented. It will then address the scope and aim of this thesis. Finally, the outline of the report is given.

1

1.1. INTRODUCTION

The offshore wind turbine industry is still in its infancy, with the first offshore wind farm installed in 1991 in Denmark. Although this is the case, the offshore wind industry is growing rapidly. The installed capacity of offshore wind farms in Europe doubled between the year 2011 and 2014, and doubled again between 2014 and 2017 [1]. There is therefore a lot of potential for improvements and space for new technologies, as the industry inherited outdated and inefficient processes and method from other sectors of the offshore industry.

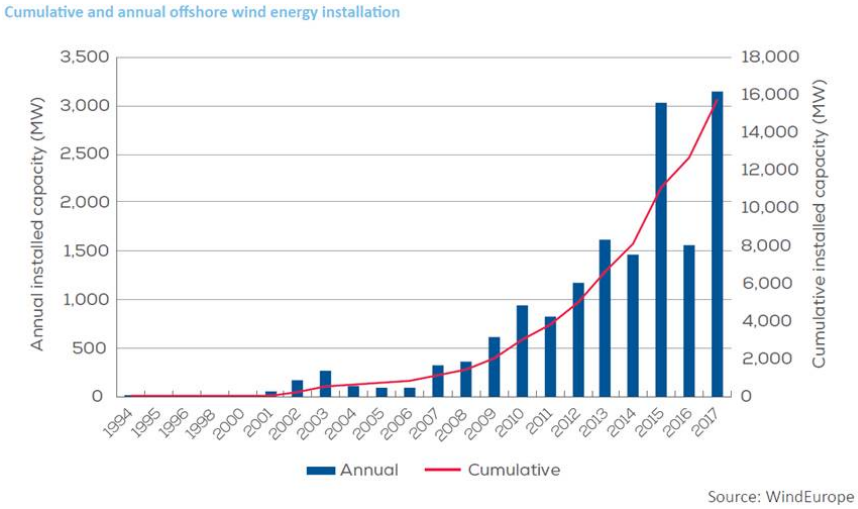

Figure 1.1: Cumulative and annual offshore wind turbine installation: WindEurope [1]

One of these procedures is the installation of offshore wind turbine rotor blades. Currently they are most commonly performed by jack-up vessels for shallow water and heavy lifting vessel for deep water. They are, however, not the best suited vessels for blade installation as they are overly dimensioned for the task. For example, the new floating offshore wind farm Hywind used the Saipem 7000 [10], a heavy lift vessel with a maximum lifting capacity of 14,000 tonnes, to install the offshore wind turbine (OWT). For the installation of the fully assembled OWT, tower + nacelle + rotor blades (±500 tonnes), this is already overqualified and is grossly over dimensioned for the maintenance or installation of a single blade. To put it into perspective the largest rotor blade currently, the LM 88.4 P with a rotor diameter of 180 meter, has a mass of only 34 tonnes. The Saipem 7000 can lift over 400 of these blades at once.

Identifying this mismatch, Temporary Works Design (TWD) saw an opportunity to design a dedicated tool for blade installation and maintenance. This tool is intended to compete with current installation methods in time and cost and has the ability to service offshore wind farms installed in both shallow and deep waters. It is therefore chosen for a concept featuring a floating solution. The resulting design after considering multiple options is shown in Figure 1.2.

The Blade Installation Tool (BIT) is a state-of-the-art solution that allows for blade installation from a floating platform. By incorporating motion compensation and decoupling it can mitigate the vessel motions, thereby reducing the relative motion between the top element of the BIT and OWT. After the BIT is connected to the tower, a blade handling kart can safely transport and install the blades to and from the nacelle.

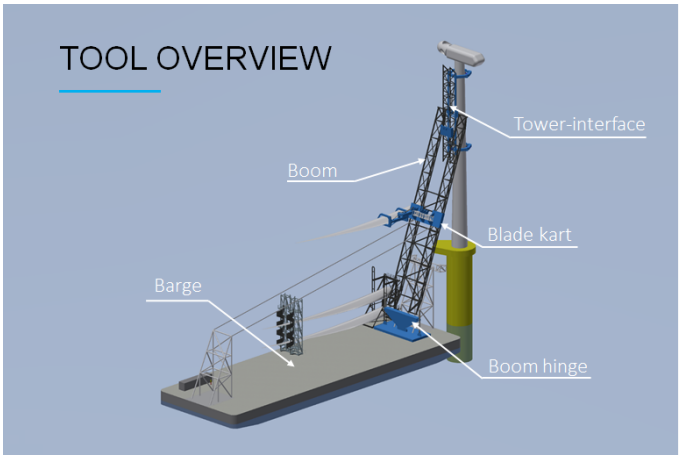

Figure 1.2: Impression image of the blade installation tool

The floating blade installation tool consists of 4 main components:

1. The boom structure, which provides support for the tower-interface and acts as a rail during the lifting operations. The boom can be adjusted in length before a project to suit different OWT heights.

2. The tower-interface is the top element of the BIT, at which the blade installation process occurs. Motion compensation and decoupling mechanisms are incorporated to mitigate the relative motions of the tower-interface and OWT, allowing the tower-interface to remain stationary, while the tool is subjected to the vessel motions.

3. The blade kart is the lifting mechanism of the BIT. It is able to move along rails installed on the boom and tower-interface. At the tower-interface it prepares the blade to be installed, adjusting for small miss alignment between rotor hub and rotor blade.

4. The blade sea-fastening provides a stable framework for blade transport and prepares the blade to be lifted by the blade kart

1

1.2. SCOPE AND AIM

The BIT is a state-of-the-art and innovative idea, consequently it is also unconventional and potential financially risky. Therefore, it is essential to perform feasibility studies to ensure the viability of the design, providing crucial information during the design process and a proof of concept to potentially interested parties. This thesis is part of the technical feasibility study, with the focus on the dynamic interaction between the BIT and OWT.

The scope of this thesis is set to the governing plane of motion, the vertical plane in the longitudinal axis of the vessel. Thus, only surge, heave and pitch vessel motions are taken into account, excluding sway, roll and yaw motions. This plane of motions is assumed to have the largest forces and motions and therefore a point of interest.

Meetings were set up between TWD and turbine manufacturers in order to get more insight in the allowable contract stresses on the blade and turbine. The following concerns were expressed with respect to the BIT and OWT interface:

- No paint damage. The tower manufacturer has to guarantee the integrity of the tower. It is therefore, one of their concern to preserve the protective paint and coating on the tower. For this reason, it is necessary to restrain the stresses acting on the tower within a certain limit. There can only be compression forces between 0 and 50 kN acting on the tower and no tension forces.

- No sliding contact. In addition to restriction on the stresses, the manufacturers want to avoid sliding contact to further ensure the protection of the tower. Fortunately, the tower-interface is designed to be stationary, thus eliminating relative motions and thereby sliding contact.

- Only horizontal loads. The tower allows for only horizontal loads, the weight of the tower-interface must therefore be fully supported by the boom. This means that the mechanical control systems must be able to support the tower-interface while also be able to compensate for the vessel motions.

The objectives for this thesis are defined with these main concerns in mind.

The main objective is to:

Gain insight in the dynamic interaction between the floating blade installation tool and OWT

The sub-questions are:

1. ***Are the interface forces on the tower acceptable in conditions comparable to the operational limits of jack-up vessels?***
   The question is posed to asses whether the BIT will be able to have similar workability as it's main competitor the jack-up vessel.

2. ***What is the relation between the vessel-tower distance and the interface forces?***
   The distance between the vessel and tower varies due to environmental conditions and mooring characteristics, as a consequence of the BIT being installed on a floating platform. This distance impacts the forces applied on the tower by the BIT. Exploring this relation gives an indication on the required capability of the mooring system and the operational sea-states.

3. ***How much does the significant wave height affect the forces and stresses on the tower?***
   This objective is set to find a relation between significant wave height of different sea-states and the forcing, giving an initial assessment of the workability of the BIT.

1

1.3. APPROACH

A dynamic model is constructed for the governing plane of motion, the vertical plane in the longitudinal axis of the vessel. The vessel undergoes the largest motions and exerts the highest forces on the OWT in this plane of motions. Only surge, heave and pitch are considered, thus excluding sway, roll and yaw motions. As This system is quite complex, a numerical method is chosen to approximate the system. A model is constructed in a step wise manner, expanding until it has the desired functionality and precision. the following steps are taken for the construction of the model.

- First component to be modelled is the BIT. The system consists of multiple bodies and constraints and thus best described using the Lagrange method. This is done using a symbolic toolpack in MATLAB based on the work of D.J. Rixen in Engineering Dynamics [11]. This method is then verified by deriving the equations of motion (EOM) for a simple system and compare it with the EOM derived with the classical mechanics method of Newton.
- Next component is the OWT, it is modelled as a cantilever beam. For this purpose, three methods are explored and evaluated, they are the finite element method (FEM), the finite difference method (FDM) and using the Lagrange method. The preferred method is used for the final model. The BIT model and OWT model are then combined by applying an interface force between the two models.
- The environmental conditions are modelled next. The environmental conditions considered are the wind, waves and current loads. The wind conditions is modelled using a spectral representation method [16]. This method generates a wind time series via a power density spectrum. The wave conditions are generated in similar fashion using the JONSWAP spectrum. The significant wave height and peak period applied in the spectrum are based on the design parameters of the system. The currents are assumed to be constant. The resulting forces from the environmental loads are computed and implemented with the rest of the model.
- The vessel motions are determined based on the first order wave forces, by applying the Response Amplitude Operators to the generated wave conditions. This is a simplified description of the vessel motions, in reality the vessel under goes motions due to second order wave drift forces, current, wind, mooring and the interaction between BIT and vessel. These effect are chosen to be neglected in accordance to the scope.
- Final part of the model is to simulate the motion compensation of the tower-interface. This is achieved by applying a force between the tower-interface and boom, which the magnitude is controlled via a PID-controller.

Using the final model, several simulations are performed under a variety of conditions to assess the BIT for the posed sub-questions. The load cases assessed are based partly on the design parameters set by TWD and party based on the objectives set by this thesis.

1.4. THESIS OUTLINE

Chapter 2; gives additional background information relating to the BIT. This will be information on the current state of the offshore wind industry, current methods used for offshore blade installation and maintenance and a full description of the principle behind the design of the BIT.
Chapter 3; elaborates on the literature and theories used for the construction of the model. it describes the Lagrange method, the three methods assessed for the OWT model and methods to generate the wind and wave conditions.
Chapter 4; describes the model. It will illustrate how the BIT and OWT is Modelled, implemented within the confine of MATLAB and finally solved using the ODE45 functionality of MATLAB
Chapter 5; shows the results gained from the simulations based on the research objectives.
And finally it ends with the conclusions, discussions and recommendations.

2

BACKGROUND INFORMATION

Two things are infinite: the universe and human stupidity; and I'm not sure about the universe.

Albert Einstein

The topic of chapter 2 is the background information for the BIT. It will first expand on the offshore wind industry and the trends it has been showing for the last decade. Next, it describes different methods currently in use for rotor blade maintenance and installation. Last it elaborates further on mechanics and operations of the BIT introduced in chapter [1]

2.1. OFFSHORE WIND INDUSTRY

The world is under threat of major climate change, the effect is already observable in the environment. Climate change is the cause behind the reduction of land ice, polar ice and sea ice, which in return strengthen the global warming. This will effect us in many ways, among them more frequent and intense heat waves, hurricanes and accelerated sea level rise. In the article [7] published in Environmental Research Letter about the consensus on climate change, shows that above 97% of the publishing climate scientists agree that the change is due to human activity of the last century. The main cause being the emission of greenhouse gasses.

In 2015, 196 parties came together under the Paris agreement to combat the climate change. Each country develops a plan appropriate to the situation of that country to reduce greenhouse gas emissions. Following the agreement, the European commission has agreed on a renewable energy target of at least 27% of the final energy consumption for 2030. This is a major driving force behind the wind energy industry both for onshore and offshore. Figure 2.1 shows that both wind and solar energy is increasing rapidly in installed capacity. Wind energy is now the second largest source of energy in Europe, only behind gas.

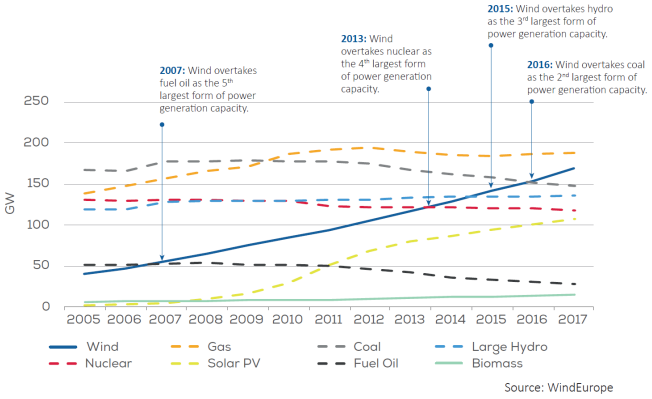

Figure 2.1: Total power generation capacity in the European Union 2005-2017: WindEurope [2]

WindEurope, an association promoting the use of wind power in Europe predicts, three scenarios for the wind industry in Europe for 2030 [3]. The central scenario predicts that 320 GW, of which 253 GW onshore and 70 GW offshore, of cumulative wind energy capacity would be installed in the EU by 2030. That would be more than double the capacity at the end of 2016 (160 GW) and over fourfold the installed capacity offshore. Even in the low scenario, assuming an unfavourable condition, it is predicted that 49 GW cumulative capacity will be installed offshore, three times the current installed capacity.

As the number of Offshore wind farms are increasing, the available space near shore decreases. That is why engineers are looking for different methods to install OWT at increasingly larger water depth. Figure 2.2 shows the increasing tendency to install wind farms at larger water depths.

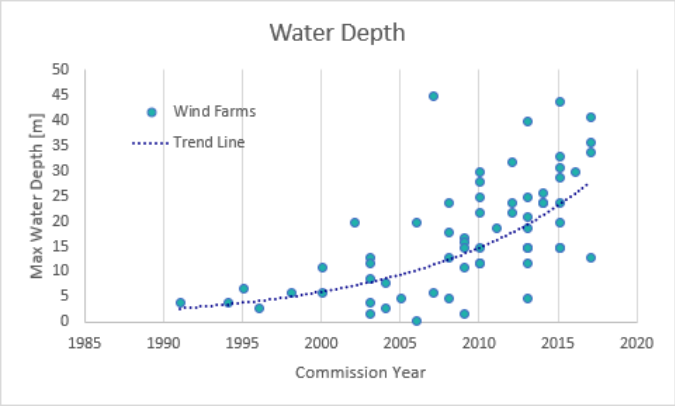

Figure 2.2: Maximum water depth of wind farms commissioned in Europe between 1991 and 2017

Most installed foundation structure for OWT is the monopile. The monopile , however, will not be suitable for the increasing water depth. That's why a lot of research and projects on the development of different floating support structure options. In 2017 it culminated in Hywind wind farm, the world first floating wind farm with a maximum water depth of 120 meters. However, not much research is done on floating installation possibilities, with the work done by K. de Groot [9] being an exceptions.

2.2. OPERATIONS AND MAINTENANCE

In the early years of the North American wind industry, there was an expectation that rotor blades would last the full lifetime of a OWT, between 20 and 25 years, without any routine inspection and maintenance. They soon realise, however, that this was not the case. Rotor blades not protected against leading edge erosion could show sign of damage after only three years [12]. Routine maintenance on a yearly basis is required in order to uphold the integrity and efficiency of the blades. According to the NREL report, 1-3% of turbines require replacement of the blades every year [15]. Therefore, in addition to routine maintenance, blades have to be replaced when failure occurs. At the end of 2017, a total of 4,149 grid connected wind turbines can be found in Europe. Consequently, this is in line with repairs between 41 and 124 turbines on a yearly basis [1].

Operations and Maintenance (O&M) can be divided into the following two main categories: minor maintenance and major maintenance [6].

Minor maintenance are tasks that are operated without the need of heavy cranes or transport of heavy equipment. These tasks include repair of electrical, control, hydraulic and sensor systems. In this case, vessels are mainly used to transport technician crews and equipment to the OWT. The advantages and disadvantages of each vessel type employed in the offshore wind maintenance industry are elaborated in Table 2.1.

Table 2.1: Comparison of vessels currently employed in the offshore wind maintenance market, source: [6]

Vessel type	Advantage	Disadvantage
Monohull	Access to turbine for Hs up to 1 meter Very high speed (25 knots)	Limited passenger (6-8) and cargo capacity No other facilities
Catamaran	Safe access to turbine for Hs up to 1.2 meter Medium speed(20)	Limited Passenger (up to 12) and cargo capacity
SWATH	Medium speed(15 knots) Passenger capacity up to 60 people	Limited cargo capacity

Minor maintenance with respect to rotor blades consists of tasks such as inspection of the blades and repainting or re-coating of the outer protection layer. These tasks are usually performed with the use of rope access method, because it requires less specialised equipment and uses relative inexpensive and readily available vessels. However, the downside of this method is that due to safety concerns for the maintenance crew, the sea sate in which rope access can be performed is limited. For reference, wind speeds up to 5 m/s are considered safe, while wind speeds between 5 and 15 m/s are risky. Wind speeds above 15 m/s are considered dangerous and thus, all maintenance activities should be ceased at this point [8]. Considering the environment in which the maintenance crew are able to operate, the repair process will be slow and less effective. As a result, it can take up to 4-5 days to manually re-coat and repaint one blade.

Figure 2.3: Rotor blade maintenance: Rope access

On the other hand, major maintenance requires heavy lifting capabilities in which vessels such as jack-ups and heavy lift vessels are used to perform these tasks. For shallow water up to 60 meters, jack-up vessels are most commonly used as these are relatively less expensive and more readily available compared to heavy lift vessels. The only option considered for OWTS installed in deep water are heavy lift vessels. In Table 2.2 the advantages and disadvantages of jack-up and heavy life vessels are summed up.

Table 2.2: Comparison of vessels currently employed in the offshore wind maintenance market for major maintenance, source: [6]

Vessel type	Advantage	Disadvantage
Jack-ups vessel	Specialisation for offshore wind farm projects	Limited operational speed
	Stable base for lifting operations	Feeder vessels required
	Cost effective in medium and high wave areas	Capability to operate up to 50m water depths
	Accommodation for both ship and maintenance crew	Time consuming due to jacking operations
Heavy lift vessel	Very flexible for unusual cargo	Low availability due to offshore oil and gas industry
	Large quantity of cargo handling	Slower mobilisation
	relatively better stability characteristics	Port entrance issues due to size
		Relative higher daily charter rates (>€ 100.000)

Figure 2.4: Wind turbine installation jack-up vessel Sea Installer

For installation and replacement, most common vessels used are jack-up vessels. These have their limitation, the 10 largest jack-up vessels currently in operation only have a maximum operation water depth of 65 meters. As mentioned earlier in the chapter, offshore wind turbine are installed at increasingly deeper water depths. Forcing the use of heavy lift vessel. the lifting capacity for both type of vessel is significant higher than the necessary capacity for lifting rotor blades.

Table 2.3: Operational water depth of the 10 largest offshore jack-up vessel

Jack-up vessel	Operational water depth
Aeolus	55 [m]
Seajacks Scylla	65 [m]
Innovation	65 [m]
Vole au vent	50 [m]
Pacific Orca	60 [m]
Pacific osprey	60 [m]
Seafox5	65 [m]
MPI Adventure	40 [m]
MPI Discovery	40 [m]
MPI Enterprise	45 [m]

Both minor and major maintenance operations have factors that can be improved on. By creating a new and cost efficient system can improve the levelized cost of energy for OWTs, taking another step in making OWT a better alternative for fossil fuel based energy generators.

2.3. TWDS FLOATING BLADE INSTALLATION TOOL

This section is omitted due to confidentiality considerations.

3

LITERATURE STUDY

Progress is made by trial and failure; the failures are generally a hundred times more numerous than the successes; yet they are usually left unchronicled.

William Ramsay

This chapter will discuss the literature on different aspects of the model. First it will elaborate on the methods used to derive the equation of motions, these are the Lagrange method and the finite element method. It will then elaborate on the three environmental conditions wind waves and current.

3.1. LAGRANGE METHOD

The formulation of the equation of motions by applying newton's law of motion, can be a cumbersome process especially for system under kinematic constraints. Each individual constraint must be considered in this method, which requires extensive mathematical manipulations. Fortunately, there is an alternative method, the Lagrange method. This method describes the position and orientation of each body with a minimum set of coordinates for which the constraints are inherently satisfied [24].

The Lagrange method has its basis in D'Alembert's form of the principle of virtual work, it allows for a formulation of the equation of motions without constraint or reaction forces. The principle of D'Alembert use the notion of virtual displacements to eliminate the constraint forces. As the constraint forces $F_{constraint}$ acts perpendicular to the path of the motion δr, its virtual work will become 0 [25].

$$F_{constraint} * \delta r = 0 \tag{3.1}$$

Instead of forces, the Lagrange method uses the energies in the system. The Lagrangian function is the difference between the kinetic energy $\mathbb{T}$ and potential energy $\mathbb{V}$. This relation allows for the derivation of the EOM for systems with out damping. The Lagrange equations can be further modified to include non-conservative forces, such as friction, with the addition of the Rayleigh's dissipation function. The formulation for the EOM becomes:

$$\frac{d}{dt}\frac{\partial \mathbb{T}}{\partial \dot{q}} - \frac{\partial \mathbb{T}}{\partial q} + \frac{\partial \mathbb{V}}{\partial q} + \frac{\partial F}{\partial \dot{q}} = Q \tag{3.2}$$

The kinetic energy $\mathbb{T}$ is defined as:

$$\mathbb{T} = \frac{1}{2} m \dot{q}^2 \tag{3.3}$$

Where $\dot{q}$ is the velocity vector of the generalised coordinates. The kinetic energy is determined for each degree of motions for each body in the system.

The potential energy $\mathbb{V}$ is the summation of every potential energies in the system. The most common potential energies considered in a dynamical system are the potential gravity energy and potential spring energy. The potential gravity energy is defined as:

$$V_{gravity} = mgq_y \tag{3.4}$$

Where m is the mass of a object g is earth's gravity and q_y is the vertical position of a mass. And the potential energy is defined as:

$$V_{spring} = \frac{1}{2} k_t q_x^2 \text{ or } \frac{1}{2} k_r q_r^2 \tag{3.5}$$

Where k is the stiffness of a translational or rotational spring. q_x and q_r are the generalised coordinates for translational and rotational displacement respectively.

The energy dissipation by non-conservative forces are adapted in the fourth term of equation 3.2. Rayleigh's dissipation function is defined as:

$$F = \frac{1}{2} c \dot{q}^2 \tag{3.6}$$

where c is the damping coefficient and $\dot{q}$ is velocity.

The last energy considered are the generalised forces Q. It can be obtained from the virtual work δW, it is given by:

$$\delta W = \sum_{i=1}^{n} F_i * \delta r_i \tag{3.7}$$

Where F is the exerted force or moment and δr_i is the virtual displacement of the body i. Taking the Jacobian of the virtual work with respect to all the generalized coordinates gives the generalised force Q.

3.2. FINITE ELEMENT METHOD

The OWT can be modelled as a cantilever beam. To be able to approximate the motion numerically, it first must be discretize. This can be performed with multiple methods. The methods considered in this thesis are the Lagrange method, finite difference method and finite element method.

Lagrange method, this method divides the beam into discrete rigid bodies jointed with rotational springs, approximating the whole cantilever beam. This approximation model can than be solved using the Lagrange method.

Finite difference method is based on Euler-Bernoulli beam formula.

$$\rho A \frac{\partial^2 w}{\partial t^2} + \frac{\partial^2}{\partial x^2}(EI\frac{\partial^2 w}{\partial x^2}) = 0 \tag{3.8}$$

Where the equation of motions for the beam is dependent on two derivatives $\frac{\partial^2 w}{\partial t^2}$ and $\frac{\partial^4 w}{\partial x^4}$. For which the latter is required to be approximated using finite difference. There are three forms in which it can be approximated, they are:

Forward difference

$$\frac{df}{dx} = \frac{f(x+h) - f(x)}{h} \tag{3.9}$$

Backward difference

$$\frac{df}{dx} = \frac{f(x) - f(x-h)}{h} \tag{3.10}$$

And central difference

$$\frac{df}{dx} = \frac{f(x+\frac{1}{2}h) - f(x-\frac{1}{2}h)}{h} \tag{3.11}$$

With central difference having the highest accuracy of the three. This method has a relative high degree of accuracy, especially compared to the rigid body method. However, it can quickly become cumbersome to implement as the system becomes more complex.

The last method explored is the finite element method. This method reduces continuous system into elements. The motions of these elements can be described using the Lagrange-Euler equation.

$$\mathbb{L} = \mathbb{T} - \mathbb{V} = \frac{1}{2}\int_l \int_a \rho V(x,y,z)^2 - \sigma(x,y,z)\epsilon(x,y,z)\, dA\, dx \tag{3.12}$$

Solving this equation requires the assumption of shapes function that describes the velocity and the deformation. After solving this equation, the motions of the full system can be described by assembling the equations of motion of each element. See Appendix B for the full derivations of the EOM using FEM. This method has, similarly to the finite difference method, a high accuracy and the added benefit that forces and boundary conditions can be applied with relative ease.

3.3. WAVE AND CURRENT

WAVE

The first environmental condition considered are the waves conditions. The wave conditions are generated using the JONSWAP spectrum. This spectrum is specifically developed for the North Sea environment, where the wave development is limited by the fetch. The waves in a fully developed conditions can be described using the Pierson-Moskowitz spectrum. This spectrum defined in the DNV Recommended Practice [18] is as follows:

$$S_{pm}(\omega) = \frac{5}{16} H_s^2 \omega_p^4 \omega^{-5} \exp^{-\frac{5}{4}(\frac{\omega}{\omega_p})^{-4}} \tag{3.13}$$

Where Hs is the significant wave height, ω_p the angular spectral peak frequency. The JONSWAP spectrum is formulated as a modification of the Pierson-Moskowitz spectrum. It is defined as:

$$S_j(\omega) = A_\gamma S_{pm}(\omega) \gamma^{\exp(-0.5(\frac{\omega-\omega_p}{\sigma\omega_p})^2)} \tag{3.14}$$

Where $A_\gamma = 1 - 0.287 \ln\gamma$ a normalizing factor and γ is a non-dimensional peak shape factor. The value for γ is 3.3 for a fully developed sea. As this is not the case, the value for γ is determined based on guidelines set by DNV [18]. it is as follows:

$$\gamma = \begin{cases} 5 & \text{for} \quad \frac{T_p}{H_s} \leq 3.6 \\ \exp(5.75 - \frac{1.15 T_p}{\sqrt{H_s}}) & \text{for} \quad 3.6 < \frac{T_p}{H_s} < 5 \\ 1 & \text{for} \quad 5 \leq \frac{T_p}{H_s} \end{cases} \tag{3.15}$$

Where σ is the spectral width parameter and is determined using DNV guidelines as well.

$$\sigma = \begin{cases} 0.07 & \text{for} \quad \omega \leq \omega_p \\ 0.09 & \text{for} \quad \omega > \omega_p \end{cases} \tag{3.16}$$

For a Hs of 2 meters and Tp of 7.75 seconds results in the spectrum shown in Figure 3.1.

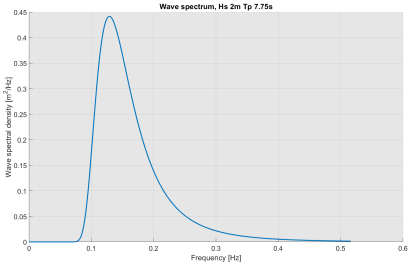

Figure 3.1: JONSWAP spectrum, with Hs 2m and Tp 7.75s

The wave condition is described for the time domain. The wave time series is generated using MATLAB with a method described by E. Branlard in Generation of time series from a spectrum [17]. The following relations are used to generate the wave time series.

$$\begin{aligned} \eta(t) &= \sum_{i=1..n} \zeta_i \cos(\omega_i t - k_i x + \phi_i) \\ \zeta_i &= \sqrt{2Sj(\omega)\Delta\omega} \\ \phi_i &= \text{random}(0, 2\pi) \end{aligned} \tag{3.17}$$

The generated wave time series are shown in Figure 3.2.

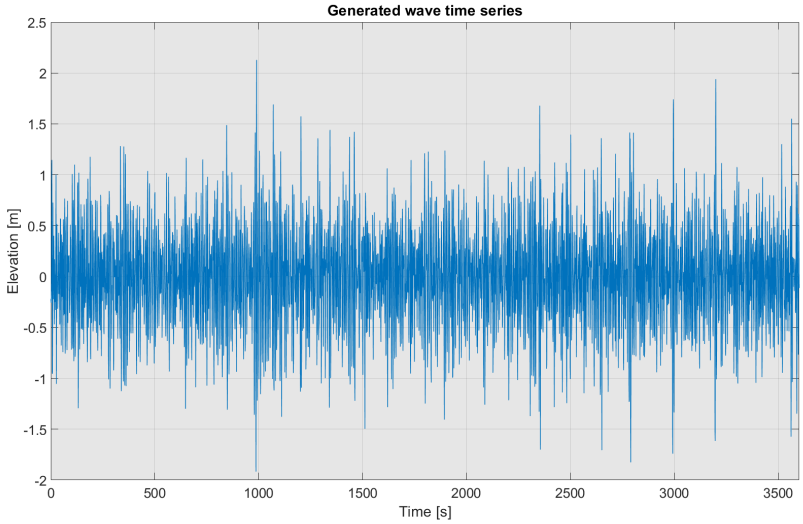

Figure 3.2: Generated wave time series

3.3.1. CURRENT

The next environmental conditions considered is current loads. The free surface current speed defined as 1.5 m/s, this is a representative current speed for the conditions in the North sea. The current profile over the water depth follows the following relations

$$V(z) = V * \frac{d_0 + z}{d_0} \quad \text{for} \quad -d_0 \leq z \leq 0 \tag{3.18}$$

Like wave velocity, the current is stretched to the actual surface elevation. This is done by Linear stretching or non-linear stretching. Linear stretching is defined by:

$$z_s = (d + \eta) * (1 + \frac{z}{d}) - d \quad \text{for} \quad -d \leq z_s \leq \eta \tag{3.19}$$

Non-linear stretching relates the water depth with Airy wave theory, it is defined by:

$$z_s = z + \eta * \frac{\sinh(k_{nl}(z+d))}{\sinh(k_{nl}d)} \quad \text{for} \quad -d \leq z_s \leq \eta \tag{3.20}$$

Where knl is the non-linear wave number. In most cases linear stretching will provide an accurate estimate of the global hydrodynamic loads and is used for this research.

3.3.2. MORISON EQUATION

The Morison equation is a semi-empirical equations to predict wave forces on an exposed vertical pile. The equations is the sum of the linear inertia force, from potential theory, and the adapted quadratic drag force, from real flows and constant currents. The results is as follows:

$$F(t) = F_{inertia}(t) + F_{drag}(t) \tag{3.21}$$

Where the inertial force can be describe with:

$$F_{intertia} = \frac{\pi}{4}\rho C_M D^2 \dot{u}(t) \tag{3.22}$$

and the drag force is described as:

$$F_{drag} = \frac{1}{2}\rho C_D D u(t)|u(t)| \tag{3.23}$$

Through the years multiple methods are developed to determine the drag and inertia constants and hundreds of researches have determine C_D and C_M, however for the purpose of this thesis the most common constant values for OWT 0.7 and 2 for C_D and C_M respectively are used. [21].

3.4. WIND

The next final environmental condition considered are is the wind. According to "Modelling and Simulation of the wind model using a spectral representation method" [16], The wind can be divided in 4 components. They are the base wind speed, gust wind speed, ramp wind speed and turbulent wind speed, see Figure 3.3 for an schematic over view of the 4 components.

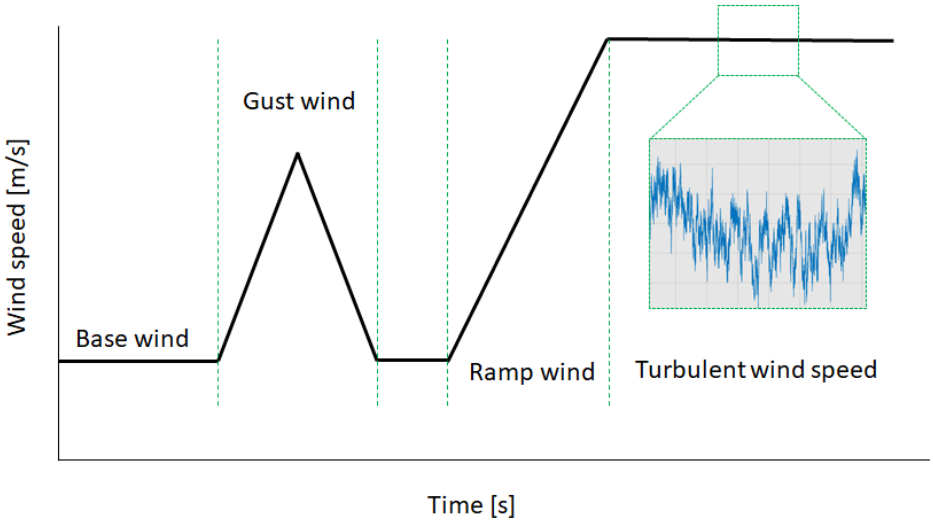

Figure 3.3: Wind component visual representation

- The base wind speed is the average wind speed. It is assumed to be constant and persistent during the entire time series.
- Gust wind speeds are sudden brief increases in wind speed. Gusts are short in duration by definition and therefore doesn't affect the mean wind speed.
- Ramp wind speed is a drastic shift in the wind speed over a short period of time.
- Turbulent wind speed is the variation of wind speed over a small-time window. It can be characterized by a power spectral.

There are a variety of spectra developed to characterise the turbulence of wind, each with different characteristics. In the offshore industry, Kármán and Kaimal spectra are most commonly used. They are described by DNV as [18]:

$$S_{Kármán} = \sigma^2 \frac{4L/U_{10}}{(1+70.8(\frac{fL}{U_{10}})^2)^{\frac{5}{6}}} \tag{3.24}$$

$$S_{Kaimal} = \sigma^2 \frac{6.868L/U_{10}}{(1+10.32(\frac{fL}{U_{10}})^{\frac{5}{3}}} \tag{3.25}$$

Where L is the integral length scale, f is the frequency, U_{10} mean wind speed and σ is the turbulence standard deviation. σ is characterized by the turbulence intensity and mean wind speed.

$$I = \frac{\sigma}{U_{10}} \tag{3.26}$$

Where I is the turbulence intensity, for offshore conditions it lies between 6 and 8 %. The integral length L is defined as:

$$L = 300\frac{z}{300}^{0.46+\frac{0.074}{\ln z_0}} \tag{3.27}$$

Alternatively, it is defined independent of the terrain roughness in IEC61400-1.

$$L = \begin{cases} 3.33z & \text{for} \quad z < 60m \\ 200 & \text{for} \quad z \geq 60m \end{cases} \tag{3.28}$$

Using the spectrum, the wind time series can be generated by means of the following equations:

$$f(t) = \sqrt{(2)} \sum_{k=k_0}^{N} \sqrt{2S(\omega_k)\Delta\omega} * \cos(\omega_k t + \phi_k) \tag{3.29}$$

The following wind time series is generated using this method:

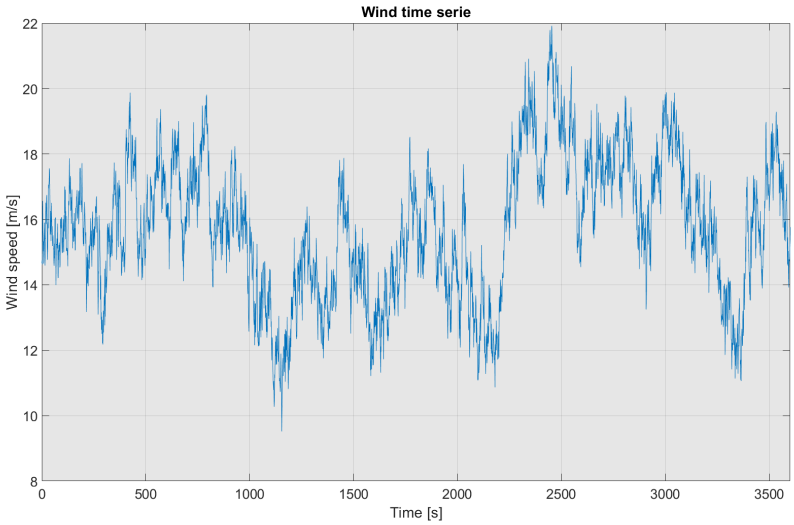

Figure 3.4: Generated wind time series

3.4.1. WIND SHEAR

The wind will vary over time, but it will vary over the height as well. Due to the friction with earth's surface wind close to the sea will be at a slower speed. There are two main models that describes the wind shear: The logarithmic profile and the power law profile. They are given in Table 3.1

Table 3.1: Wind profile due to shear

Logarithmic profile	Power law profile
$V_w(z) = V_{w,r} * \frac{\ln(\frac{z}{z_0})}{\ln(\frac{z_r}{z_0})}$	$V_w(z) = V_{w,r} * \left(\frac{z}{z_r}\right)^{\alpha_{shear}}$

$V_{w,r}$ = the wind speed at reference height
z = height
z_0 = the surface roughness length
z_r = height of the reference wind speed
α = power law coefficient dependent on the terrain type

DNV describes a list of typical roughness parameter values for different terrain types. Table 3.2 shows a few roughness parameters

Table 3.2: Roughness parameters according to DNV-RP-C205 [18]

Terrain type	Roughness parameters z_0 [m]	Power-Law exponent α
Plane ice	0.00001-0.0001	
Open sea without waves	0.0001	0.12
Open sea with waves	0.0001-0.01	
Coastal areas with onshore wind	0.001-0.01	
Snow surface	0.001-0.006	
Forest and suburbs	0.3	0.3
City centres	1-10	0.4

3.4.2. WIND FORCE

The wind force is computed using the following draq equation:

$$F_{wind} = \frac{1}{2} C_s \rho A U^2 \tag{3.30}$$

Where C_s is the drag coefficient depending on the shape of the object, ρ is the density of air, A is the cross sectional area and U is the wind speed. Table 3.3 shows a list of different drag coefficients for a variety of shapes.

Table 3.3: Shape coefficient, drag according to GL IV 6-4

Shape	Cs
Spherical shapes	0.4
Cylindrical shapes (all sizes)	0.5
Large flat surface	1
Drilling derrick	1.25
Wires	1.2
Exposed beams and girders under deck	1.3
Small parts	1.4

Open truss structural components, such as lattice structures, derrick tower, crane booms can be approximated by taking 60% of the projected area and a drag coefficient of 1.25, effectively using a drag coefficient of 0.75.

4

DYNAMIC MODELLING OF THE BIT AND OWT

A man who dares to waste one hour of time has not discovered the value of life.

Charles Darwin

This chapter describes the dynamic model used to simulate the motions of the system. It goes into detail on each component of the model, they are as follows. The first component considered is the BIT and how it is implemented using the Lagrange method. Next it assesses three methods to model the OWT. Then it elaborates the environmental conditions considered. Further, it discusses the vessel model. And finally, goes into detail how to integrate each component into a single model.

4.1. INTRODUCTION

To be able to assess interaction between the BIT and OWT dynamically, it is necessary to create a model of the system. The system is divided into four components, each is first modelled separately and then integrated into a single model. The four components are the model for the BIT, OWT, environmental conditions, and vessel motions. A schematic view of the components can be seen in Figure 4.1.

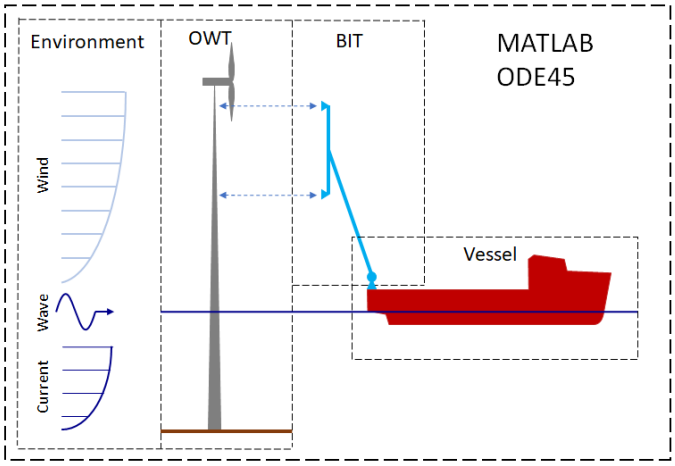

Figure 4.1: Schematic view of the system

The first component modelled is the BIT. Because the system is under several constraints and consist of multiple bodies, it is best to define the EOM with the Lagrange method.
The second component of the model is the OWT. The OWT is modelled as a cantilever beam, with the fixed end at the mud line and the hub at the free end. Three methods are explored to model this, the results are discussed later in this chapter.
Next component of the model is the environmental conditions. Wind, waves and wind are considered for this thesis. Wind loads are applied on the OWT and BIT. Current load is only applied on the tower. And the vessel is only subjugated to wave loads.
The last component is the vessel motions. The vessel motion is determined using the RAO characteristics of the Siem Moxie. The resulting vessel motions are then transposed to the motions of the boom base.
Finally, every component is integrated into a single model. This is done within the frame work of MATLAB. The integrated model can then be simulated under different load cased, this is done using the ODE45 functionality of MATLAB.

4.2. BLADE INSTALLATION TOOL MODEL

The first component, the BIT, is modelled using the Lagrange method. This is implemented in MATLAB with a method used by D.J. Rixen in his example for Engineering Dynamics [11], Dynamic analysis of a "fun bike". The method uses the symbolic tool pack of MATLAB to derive the EOM with the computer instead of manually performing the derivations. The following sections goes further into detail how the BIT is modelled using this method.

4.2.1. GENERALISED COORDINATES

The first step in the Lagrange method is to define the generalised coordinates. They are selected such that constraints are inherently satisfies, resulting in a minimum set of coordinates. The generalised coordinates selected for the BIT are shown in Figure 4.2

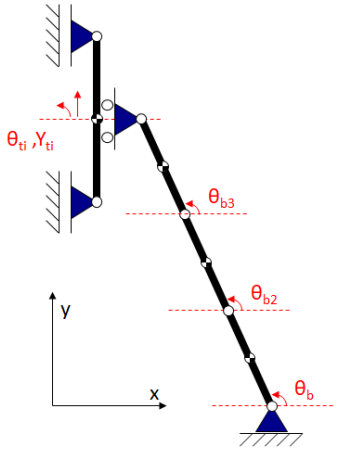

Figure 4.2: Generalised coordinates of the blade installation tool

The tower-interface has two DOFs, which are specified by the rotation and vertical displacement. The horizontal displacement is constraint by the boom and therefore not defined as a generalised coordinate.
The boom is discretized into three rigid elements, each element can pivot around the joint or hinge, resulting in three degree of freedom. This is done to consider the bending of the boom; more elements would result in higher accuracy. However, each additional element will increase the computational requirements drastically. With three elements it is possible to approximate the first 2 bending modes of the boom. This is assumed to be enough as the boom has a relative high bending stiffness.

4.2.2. KINEMATIC RELATIONS

The next step in the Lagrange process is to define the kinematic relation, descriptions of the position and orientation of each element dependent on the generalised coordinates. The velocity of the bodies can be derived using the following equation.

$$\begin{bmatrix} \dot{X}_1 \\ \dot{X}_2 \\ \vdots \\ \dot{X}_n \end{bmatrix} = \begin{bmatrix} \frac{\partial X_1}{\partial q_1} & \frac{\partial X_1}{\partial q_2} & \cdots & \frac{\partial X_1}{\partial q_n} \\ \frac{\partial X_2}{\partial q_1} & \frac{\partial X_2}{\partial q_2} & \cdots & \frac{\partial X_2}{\partial q_n} \\ \vdots & \vdots & \ddots & \vdots \\ \frac{\partial X_m}{\partial q_1} & \frac{\partial X_m}{\partial q_2} & \cdots & \frac{\partial X_m}{\partial q_n} \end{bmatrix} * \begin{bmatrix} \dot{q}_1 \\ \dot{q}_2 \\ \vdots \\ \dot{q}_n \end{bmatrix}$$

Where X_i are the position and orientation relations, q_i are the generalised coordinates and $\dot{q}_n$ is the generalised velocity.

4

4.2.3. ENERGY

With the kinematic relations defined, it is possible to describe the energies in the system. The different kind of energies are described in section 3.1. Figure 4.3 shows an overview of the springs and dampers considered for the BIT.

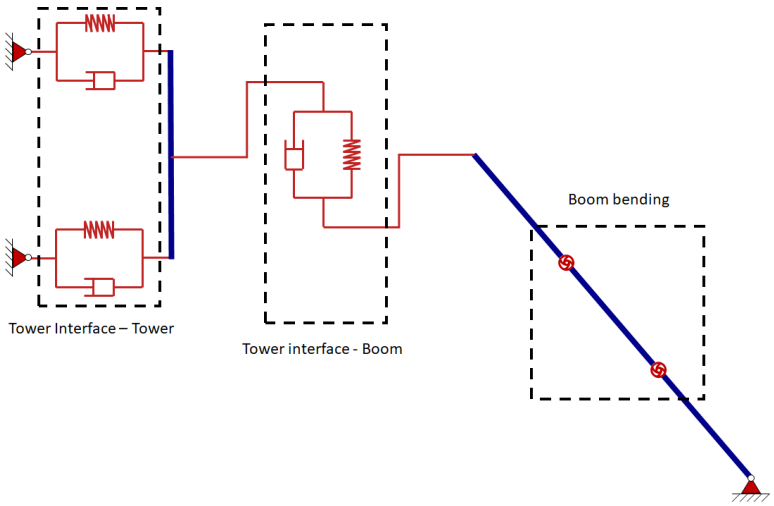

Figure 4.3: Diagram of the energy components of the BIT

The bending of the boom is approximated with rotational springs and dampers. The spring and damper coefficient used computed based on the design of the BIT, they are $3.9 * 10^{10}$ and 1% The vertical interaction between tower-interface and boom is initially modelled as a spring and damper with the coefficient comparable to the hydraulic cylinder. These are replaced at the later stage with a generalised force, of which the magnitude is controlled with a PID controller. The tower-interface and tower interaction are modelled by two sets of spring dampers.

4.2.4. DETERMINE THE EOM

The final step is to determine the equation of motions and thereby the mass and stiffness matrix. This is done using the Lagrange equation:

$$\frac{d}{dt}\frac{\partial \mathbb{T}}{\partial \dot{q}} - \frac{\partial \mathbb{T}}{dq} + \frac{\partial \mathbb{V}}{\partial q} + \frac{\partial F}{\partial \dot{q}} = Q$$

The terms in the Lagrange equations are determined as follows:

$$\begin{aligned}
\frac{\partial \mathbb{T}}{\partial \dot{q}} &= \text{Jacobian}(\mathbb{T}, \dot{q}) \\
\frac{d}{dt}\frac{\partial \mathbb{T}}{\partial \dot{q}} &= \text{Jacobian}(\frac{\partial \mathbb{T}}{\partial \dot{q}}, t) + \text{Jacobian}(\frac{\partial \mathbb{T}}{\partial \dot{q}}, q) * \dot{q} + \text{Jacobian}(\frac{\partial \mathbb{T}}{\partial \dot{q}}, \dot{q}) * \ddot{q} \\
\frac{\partial \mathbb{T}}{\partial q} &= \text{Jacobian}(\mathbb{T}, q) \\
\frac{\partial \mathbb{V}}{\partial q} &= \text{Jacobian}(\mathbb{V}, q) \\
\frac{\partial \mathbb{F}}{\partial \dot{q}} &= \text{Jacobian}(F, \dot{q}) \\
\frac{\partial Q}{\partial q} &= \text{Jacobian}(Q, q)
\end{aligned} \tag{4.1}$$

Where $\mathbb{T}$ is the kinetic energy, $\mathbb{V}$ is the potential energy,F is the dissipation function and Q is the generalised force. The matrix follows from these relations, the term dependent on the accelerations. In this case it is described by Jacobian($\frac{\partial \mathbb{T}}{\partial \dot{q}}, \dot{q}$).

4.3. OFFSHORE WIND TURBINE

The OWT is modelled as a cantilever beam, this can be preformed by a variety of methods. The methods considered are the finite element method (FEM), finite difference method (FDM) and Lagrange method. Each method is applied for a static load case and compared with the analytical results in order to asses which method is preferred. The load case considered, as seen in Figure 4.4, is a 100 meter cantilever beam under a horizontal load of 10 kN at the free end.

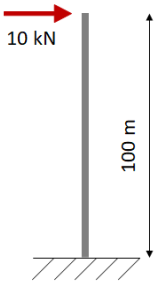

Figure 4.4: Tower comparison load case

The first comparison uses 10 elements or 11 nodes for each method, the results can be seen in Figure 4.5. It can be seen that FEM gives a results exactly matching the analytical results, the results of FDM is slightly off and Lagrange method has the worse accuracy of the three methods.

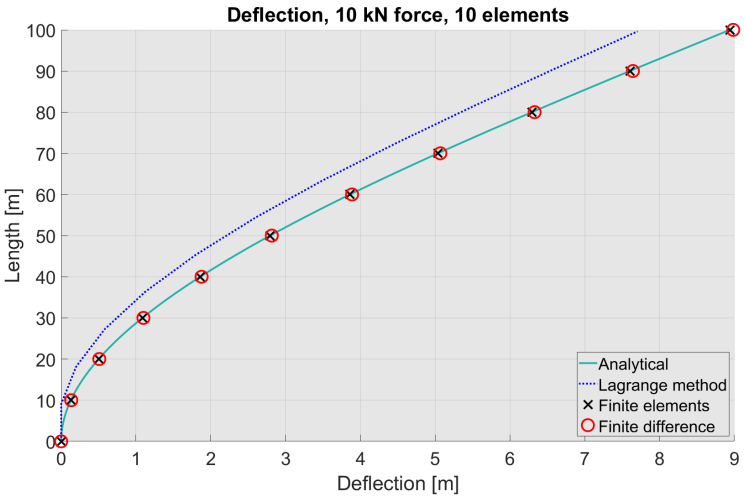

Figure 4.5: Tower model comparison with 10 elements

In the second comparison, 20 elements are used for FEM and FDM and 100 elements for the Lagrange method, the results can be seen in Figure 4.6. FEM and FDM have similar results at these number of elements, this is to be expected as FEM has twice the DOFs compared to FDM. The results of the Lagrange method are still off the analytical results, even at 100 elements.

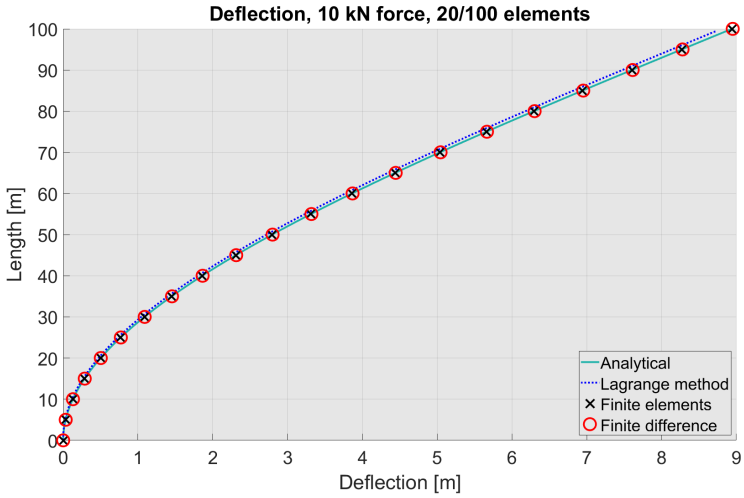

Figure 4.6: Tower model comparison with 20 and 100 elements

The Lagrange method results in the lowest accuracy of the three methods, even with significant more elements. However, using the Lagrange method to model the OWT means that the BIT and OWT is described using the same method, resulting in a less complex model. Further, the Lagrange method allows for an easy implementation of the gravitational effects. Nevertheless, this does not compensate for the significant reduction in accuracy, for this reason the Lagrange method is not used to model the OWT.

FDM has a lower accuracy than FEM but is faster to compute. Although slightly different both methods have similar results. Considering this, FEM is preferred as it has an edge over FDM in the ease of implementing the boundary conditions.

There is a trade-off between accuracy and computational requirements. The accuracy of the model can be increased by increasing the number of nodes, but this also increases the time and computations required. For the model 15 elements are used, this allows for a relative accurate result with FEM, while limits the required computational time.

The model of the OWT assumes a continuous structure from the mud line to the hub, thus ignoring the transition between the monopile and tower, as well as the transition piece. The dimensions used are based on the Vestas 3MW turbine at Northwind offshore wind farm, located in the North Sea at a water depth of approximately 30 meters. The dimension of each element is adjusted to reflect the diameter and wall thickness of the OWT, by taking the average over the length of the element, resulting in a step wise tapering of the OWT model.

4.4. ENVIRONMENTAL FORCES

Three environmental loads are considered, they are loads resulting from wind, waves and current. The method to generate these loads are described in the literature study in chapter [3]. This section further elaborates on the parameters used and the method how these forces are exerted on the rest of the model.

4.4.1. WIND

The first environmental condition considered is the wind. Wind plays a large roll in the workability of the BIT, as the BIT has to operate at wind conditions comparable to the operability limits of jack-up vessels. Therefore, to determine the viability of the BIT, a wind time series is generated using an average wind speed of 16 m/s. The wind loads are computed based on the element on which the force is applied and the wind speed at that point in space and time. The coefficient used are described in GL's Rules for classification and construction [19]. Table 4.1 shows the coefficient used.

Table 4.1: Wind coefficient for different model elements, source [19]

Model component	coefficient
Tower (Cylindrical shape)	0.5
Boom (truss work)	1.25 * 60%
Rotor blade (flat side)	1.5

The wind loads are only considered for the OWT, boom and the drag component of the rotor blade, thus loads on the tower-interface, vessel and surface friction and lift of the blade are neglected.

- The wind forces on the tower-interface is neglected, because it is assumed that due to the proximity of the tower-interface and tower that the wind is shielded by the tower.
- Surface friction of rotor blades are neglected with the assumption that these forces is relative small.
- Wind forces for the vessel are neglected because it falls out of the scope of this thesis. This thesis does not model the station keeping of the vessel, therefore it does not consider the vessel motion under wind loads.

4.4.2. WAVE AND CURRENT

Similar to the wind conditions, the wave conditions are determined based on the operability of the jack-up vessel. The operational Hs limit of jack-up vessel lies in the range between 1.5 meter and 2 meter, for which wave time series are generated to perform the simulations.

The current speed is based on the average current speed of the north sea, 1.5 m/s. For the reason elaborated in the wind section 4.4.1, the current conditions is only applied for the OWT.

The load generated by the wave and current are determined using the Morison equations. The drag and inertia coefficient used are 0.7 and 2 respectively, these are commonly used coefficient for the Morison equation [21].

4.4.3. REDUCING SIMULATION TIME

Common practice in the offshore industry is to simulate dynamics system for 3 hours. Due to the restriction of time and resources, the simulation time has been reduced to 1 hour. This will change the probable maximum and minimum wave and wind amplitude due to the reduction of time. To be conservative in the results, the environmental conditions are generated for 3 hours and a interval of a hour with the largest wave and wind amplitude are chosen for the simulation.

4.5. VESSEL MOTIONS

The last model component is the vessel motion. The vessel motions are derived directly from the wave conditions using the response amplitude operator (RAO) of the vessel Siem moxie. As a consequence, the current loads, wind loads and second order wave drift forces are neglected. The Siem moxie is an offshore supply vessel, which, among other things, has done work on the Hywind wind farm. The RAO characteristics of this vessel is acquired using ShipX hydrodynamic software. This software uses strip theory, to compute the RAO. The acquired RAO for surge, heave and pitch are shown in Figure 4.7.

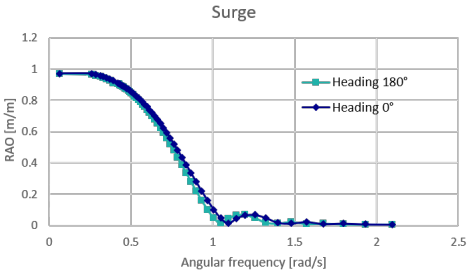

(a) Surge RAO

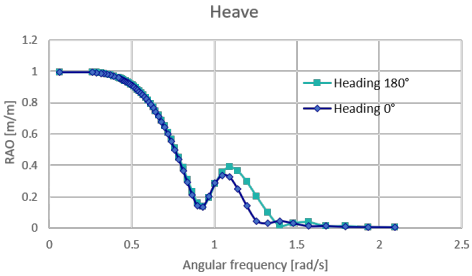

(b) Heave RAO

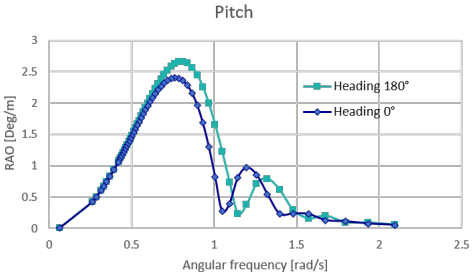

(c) Pitch RAO

Figure 4.7: The surge, heave and pitch RAO for the vessel Siem Moxie

Wave conditions resulting in the highest accelerations for the vessel are used to assess the operability of the BIT. This is achieved by determining the peak period at which the vessel has the highest response. For this purpose, three periods are examined, they are 7.75, 12 and 200 seconds. At the peak period of 7.75 seconds occurs the highest pitch response, at 200 seconds the largest surge and heave response occurs and at 12 seconds is a combination response of all three motions. The vessel motions at the boom base undergoes the largest acceleration at the peak period of 7.75.seconds. This can be expected as the vessel under goes the largest displacement at 200 seconds but at a very low speed and acceleration. Therefore, only the peak period of 7.75 is used for the simulations.

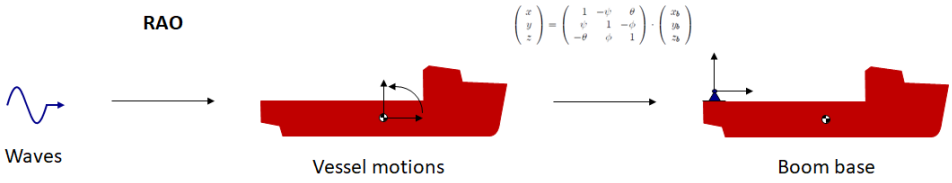

Figure 4.8: Schematic steps in the vessel motion modelling

Figure 4.8 shows the steps to determine the motions of the boom base. First the vessel motions are determined by applying the RAO on the generated wave series. This is done for each wave component, ensuring that the same wave is applied on the OWT and on the vessel. The resulting surge, heave and pitch motions are then transposed to the motions of the base through the following relations:

$$\begin{aligned} X_{base} &= X_{vessel} + y_p * \theta \\ Y_{base} &= Y_{vessel} - x_p * \theta \end{aligned} \tag{4.2}$$

Where $\theta, X_{vessel}, Y_{vessel}$ are the pitch, surge and heave motions respectively and $y_p$andx_p are the x and y position of the boom base in relation with the centre of gravity. These relations hold for small pitch angles.

4.6. INTEGRATED MODEL

The final step is to integrate every component into one single model. The state-space is required to be able to simulate the motions of the system. The state-space is the position and velocity vector of every DOF of the system. Using numerical methods it is possible to determine the state-space of the next time step, by integrating the time derivative of the state-space over time. The time derivative of position and velocity is the velocity and acceleration. The velocity is already known as it is included in the state-space, only the accelerations have to be determine. This is done using the EOM determined for the BIT and OWT. By dividing the force vector with the mass matrix results in the acceleration vector.

4.6.1. INTERFACE FORCES

Due to the different method used to determine the EOM of the BIT and OWT it is necessary to introduce interface forces. For the BIT model this is already incorporated in the formulation of the EOM, the interface forces are introduced as energies, dependent on the position of the OWT and BIT. In contrast, for the OWT model, this force requires to be computed separately and introduced as an external force, also dependent on the position of the OWT and BIT.

4.6.2. PID CONTROLLER

Up to this point, the interaction between the tower-interface and boom is modelled as a spring and damper as a place holder. To be able to more accurately model the motion compensation system, the spring and damper are substituted with a generalised force, of which the magnitude of the force is determined by a PID controller.
The PID controller is tasked to maintain the vertical position of the tower-interface in relation to the OWT. This is achieved with the proportional, integral and derivative elements of the controller. The proportional element is determined by the relative vertical position between the tower-interface and the tower. The derivative element is determined by the velocity of the tower-interface. And the integral element is determined by the integration of the error over time. This is performed by providing the error as a component of the state-space, which the ODE function, explained in the next section, integrates it over time.

4.6.3. ODE FUNCTION

The numerical integration process is done using the ODE45 function of MATLAB. This function used the Runge-Kutta method to solve the ordinary differential equations. By supplying the initial state-space and the time differential of the state-space to ODE45 functions, it can compute the subsequent state-spaces. If the time step is undefined the function will adjust the time step between integrations until the results are within a certain precision threshold.

5

RESULTS

The good thing about science is that it's true whether or not you believe in it.

Neil deGrasse Tyson

Simulations are performed for different load cases to asses the sub-questioned posed in this thesis. The results from these simulations are presented in this chapter.

5.1. INTERFACE FORCES IN CONDITIONS COMPARABLE TO THE OPERATIONAL LIMITS OF JACK-UP VESSELS

Simulations are performed to asses the dynamic interaction between the BIT and OWT, to asses whether the interface forces remain within the allowable limits under environmental conditions comparable to the operational limits of jack-up vessel. For this purpose 6 lifting phases during the operations are considered, they are:

- Phase (a), not lifting. The blade is not yet lifted onto the BIT. This simulation is used as a base line for the other load cases.
- Phase (b), The blade is midway up the boom. At this point the blade creates the largest deflections on the boom.
- Phase (c), The blade is at top of the boom. This is highest point of the boom before the blade is lifted onto the tower-interface
- Phase (d), The blade is at the tower-interface with the blade in horizontal position. The largest moment due to gravity occurs in this state.
- Phase (e), The blade is at the tower-interface with the blade at an angle of 45 °. Lowering the angle of the blade lowers the moment acting on the tower-interface.
- Phase (f), The blade is at the tower-interface with the blade in vertical position. At this stage the moment due to the gravity acting on the blade is eliminated.

For each load case, simulations are performed for a Hs of 1.5 meter and 2 meter, 0° and 180 ° heading.

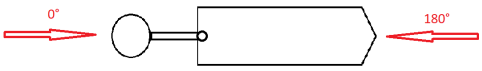

Figure 5.1: Heading convention

See Table 5.1 for an summary of the important parameters used for the simulation of the load cases.

Table 5.1: Load case parameters

Category	Input
Significant wave height	1.5 - 2 meters
Peak period	7.75 seconds
Heading	0° & 180°
Distance OWT to Vessel	10 meters
Water depth	30 meters
OWT	3MW turbine with 84 meters Hub height
Lifting phases	6 phases

The 6 lifting phases are shown in the Figure 5.2

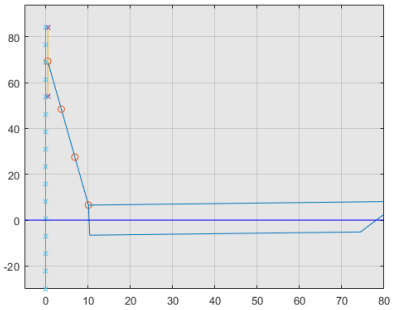

(a) Not lifting

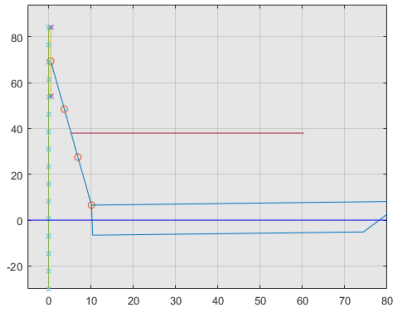

(b) Midway boom

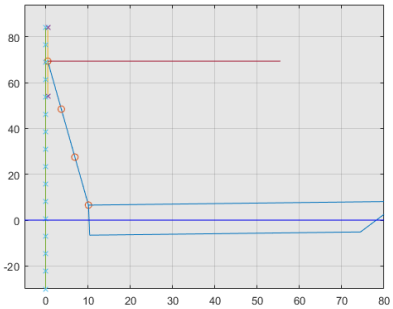

(c) Top boom

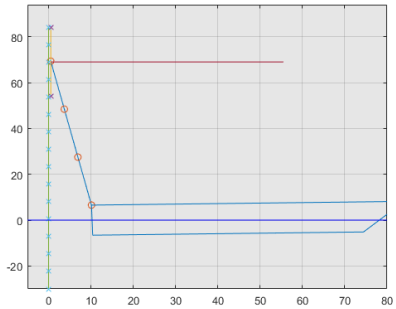

(d) Tower-interface horizontal

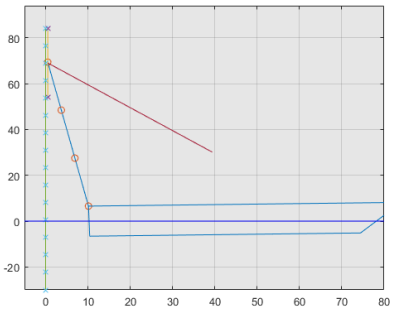

(e) Tower-interface 45°

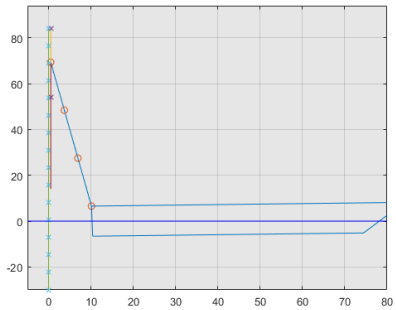

(f) Tower-interface vertical

Figure 5.2: 6 Lifting Phases

See appendix A for the full results of the time domain simulations. The following section highlights some of the note worthy results.

Figure 5.4 shows the top interface forces between BIT and OWT, for the three lifting phases (a) not lifting, (b) mid boom and (c) top boom for the load case of 2 Hs and 0° heading. The red lines represents the forcing range for which these forces should be remain within. Figure 5.5 shows the bottom interface force under the same conditions.

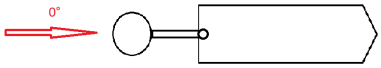

Figure 5.3: 0° heading

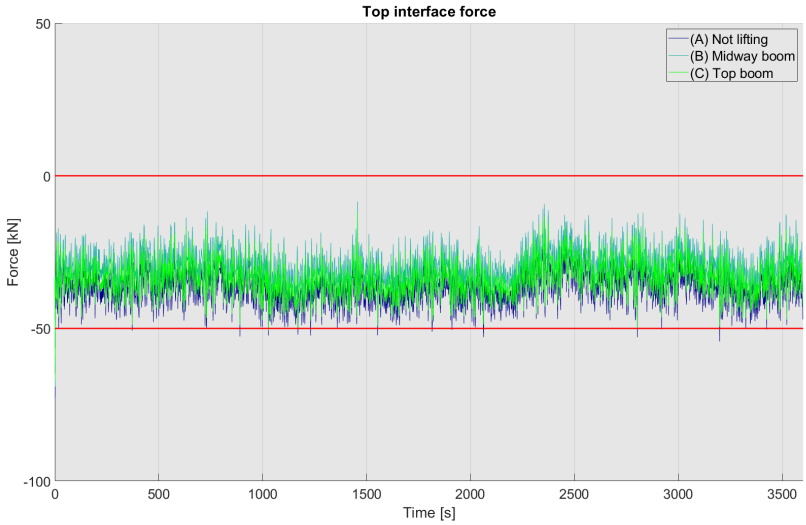

Figure 5.4: Top interface forces comparison for the lifting phases (a), (b) and (c) for heading 0° and Hs 2m

Table 5.2: Force values of the simulations for heading 0° and Hs 2m

Top interface forces				
Lifting Phase	Mean force [kN]	Max force [kN]	Min Force [kN]	Force range [kN]
No blade	-36.7	-14.7	-54.3	39.5
Midway boom	-29.2	-8.5	-45.5	37.1
Top boom	-33.4	-12.0	-50.6	38.6

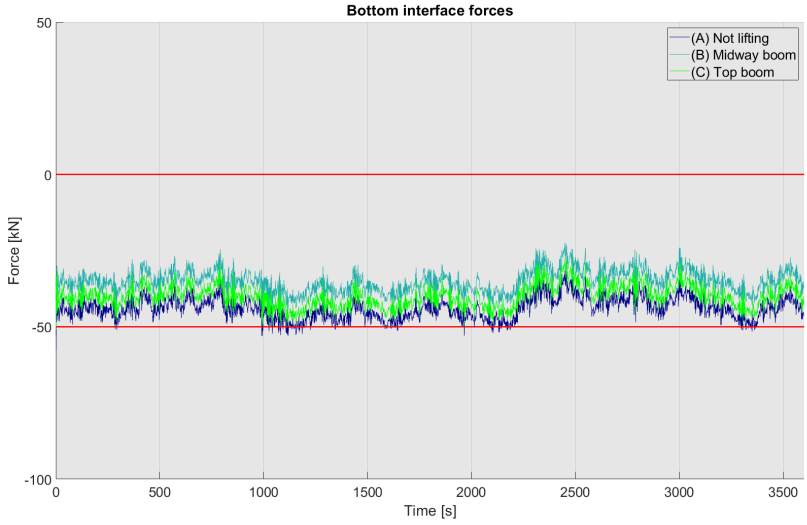

Figure 5.5: Bottom interface forces comparison for the lifting phases excluded the phase at which the blade is at the tower-interface for heading 0° and Hs 2m

Table 5.3: Force values of the simulations for heading 0° and Hs 2m

Bottom interface forces				
Lifting Phase	Mean force [kN]	Max force [kN]	Min Force [kN]	Force range [kN]
No blade	-43.9	-31.4	-53.0	21.7
Midway boom	-34.9	-22.4	-45.0	21.7
Top boom	-39.9	-27.2	-50.3	23.1

There are several aspect to remark upon. The forces of the three lifting phases are relative close to each other. The difference between the three lies at the mean of the forcing. This can be expected as the blade will create a turning moment, reducing the force against the tower. What can also be seen is a peak force at the beginning of the simulation, this is due to the initial conditions determined for the simulation. This peak will be ignored for the rest of the analysis.

The following two figures, Figure 5.6 and Figure 5.8 show the top and bottom interface of the same three lifting phases as the previous figures, with an environmental heading of 180 °. As can be expected the forces follows the same pattern, with only the amplitude reversed relative to the mean. The biggest difference is the average force, for the heading of 180 ° the pressure force is increased with 28 kN for the top interface forces and 17 kN for the bottom interface forces.

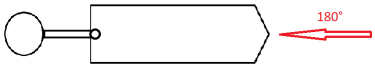

Figure 5.6: 180 ° heading

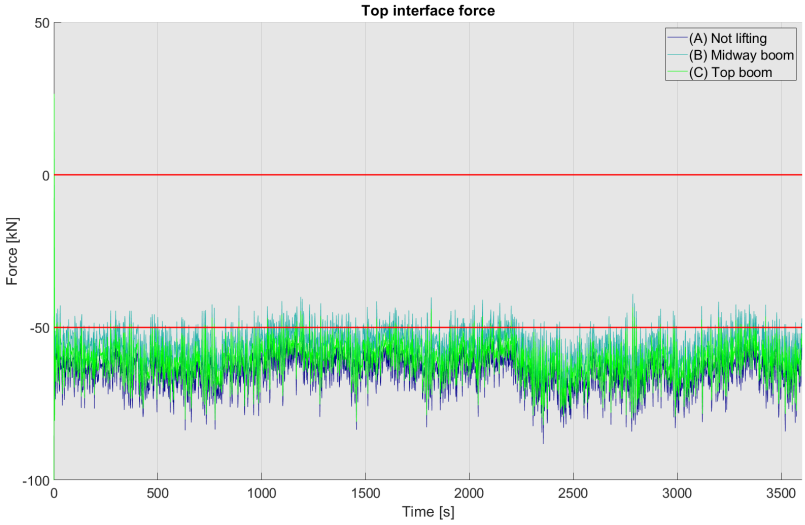

Figure 5.7: Top interface forces comparison for the lifting phases excluded the phase at which the blade is at the tower-interface for heading 180° and Hs 2m

Table 5.4: Force values of the simulations for heading 180° and Hs 2m

Top interface forces				
Lifting Phase	Mean force [kN]	Max force [kN]	Min Force [kN]	Force range [kN]
No blade	-64.8	-47.3	-88.2	40.9
Midway boom	-56.2	-39.0	-77.3	38.3
Top boom	-61.3	-43.4	-82.0	38.6

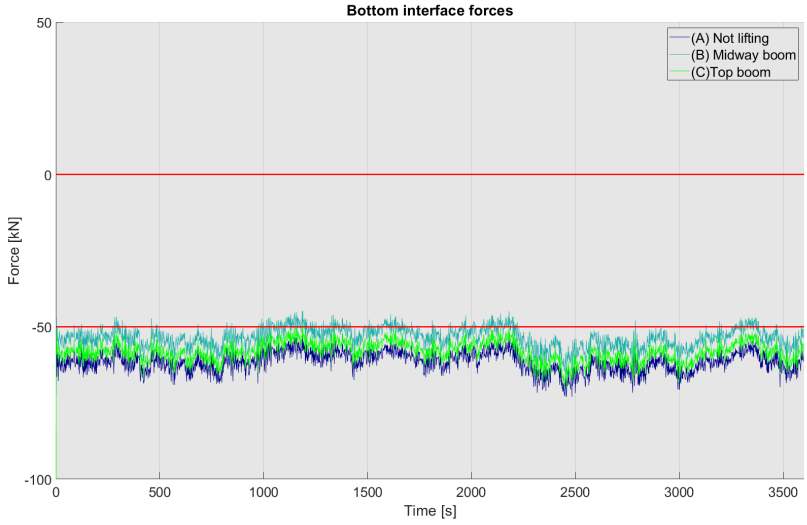

Figure 5.8: Bottom interface forces comparison for the lifting phases excluded the phase at which the blade is at the tower-interface for heading 180° and Hs 2m

Table 5.5: Force values of the simulations for heading 180° and Hs 2m

Bottom interface forces				
Lifting Phase	Mean force [kN]	Max force [kN]	Min Force [kN]	Force range [kN]
No blade	-61.7	-53.1	-73.0	20.0
Midway boom	-53.5	-44.7	-65.6	20.9
Top boom	-58.3	-49.3	-70.3	20.9

Although the interface forces do not lie within the allowable range, the mean forces can be reduced by either closing the distance between vessel and tower or via winches to reduce the load on the tower.

The following three Figures 5.9, 5.10 and 5.11 show the top and bottom interface forces for the lifting phase where the blade is fully loaded onto the tower-interface. The blades are under different angles, 90 °45°, 0°respectively.

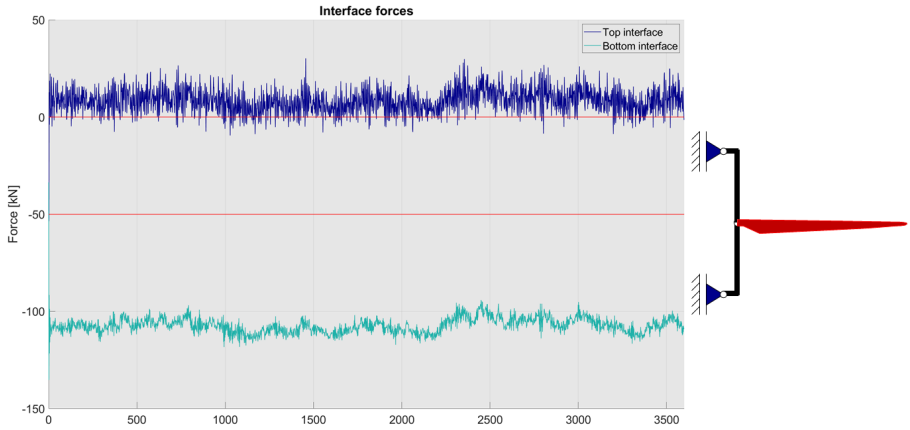

Figure 5.9: Simulation parameters: Hs 2 meters, Heading 0°, Blade at the tower-interface at an angle of 90 °.

The moment of the blade due to gravity is applied to the tower-interface. The only mechanism to counteract this moment is through the tower-interface forces. This explains the large difference between the two forces. The results is that the two interface forces will not be restricted within the allowable range. The moment of the blade can be reduced by lowering the angle of the blade. This reduces the difference between the top and bottom interface. However, due to the position of the blade, additional wind loads will be introduced to the blade. This can be seen in the Figures 5.10 and 5.11. Under an angle of 45 ° the difference between the forces are still larger than 50 kN. When the blade angle is reduced to 0 ° the force range will exceed 50 kN due to the wind loads.

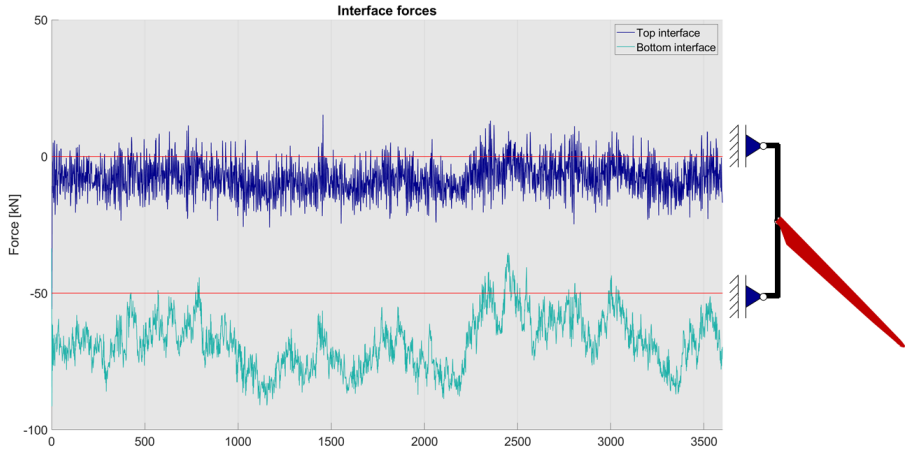

Figure 5.10: Simulation parameters: Hs 2 meters, Heading 0°, Blade at the tower-interface at an angle of 45°

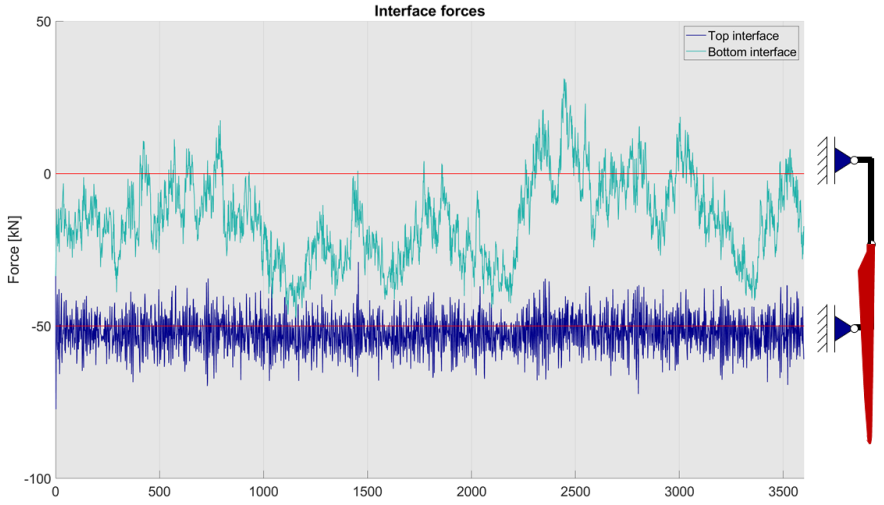

Figure 5.11: Simulation parameters: Hs 2 meters, Heading 0°, Blade at the tower-interface at an angle of 0°

5.2. VESSEL OWT DISTANCE

Simulations with different distances between the OWT and vessel are performed to determine the relation between the interface forces and the OWT-vessel distance. For the lifting phase (A), not lifting, the OWT-vessel distances are varied between 5 and 27.5 meters with an interval of 2.5 meters. See Figure 5.12 and 5.13 for the resulting top interface force from the simulations.

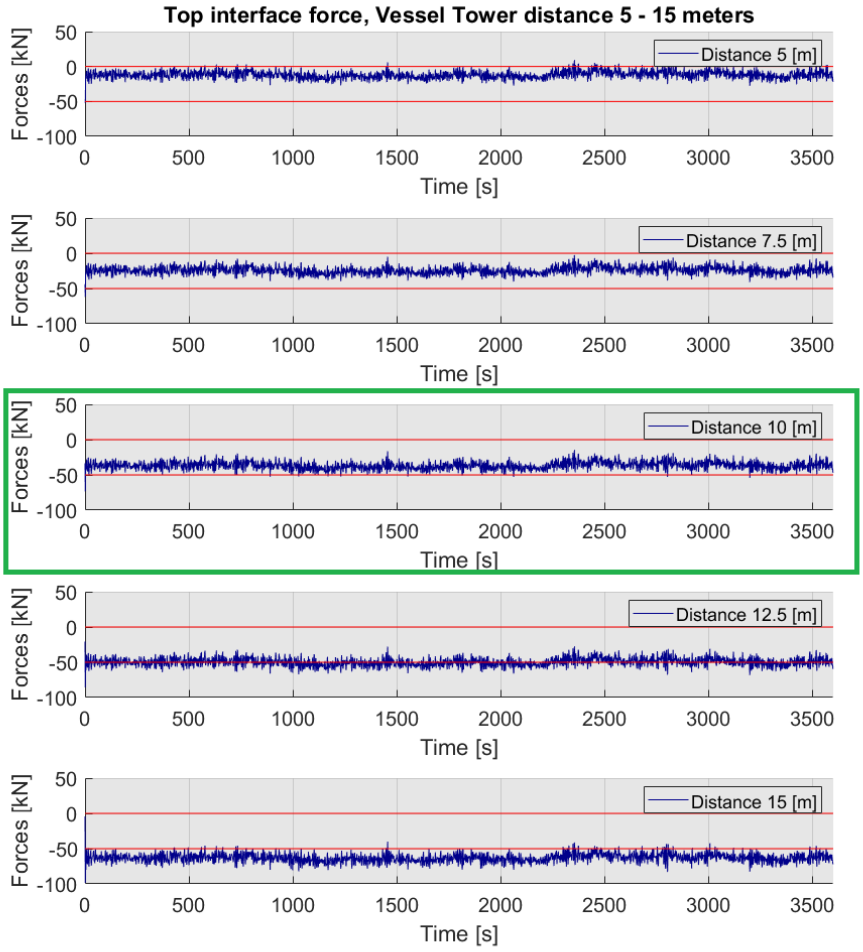

Figure 5.12: Top interface force for vessel and tower distance between 5 and 15 meters

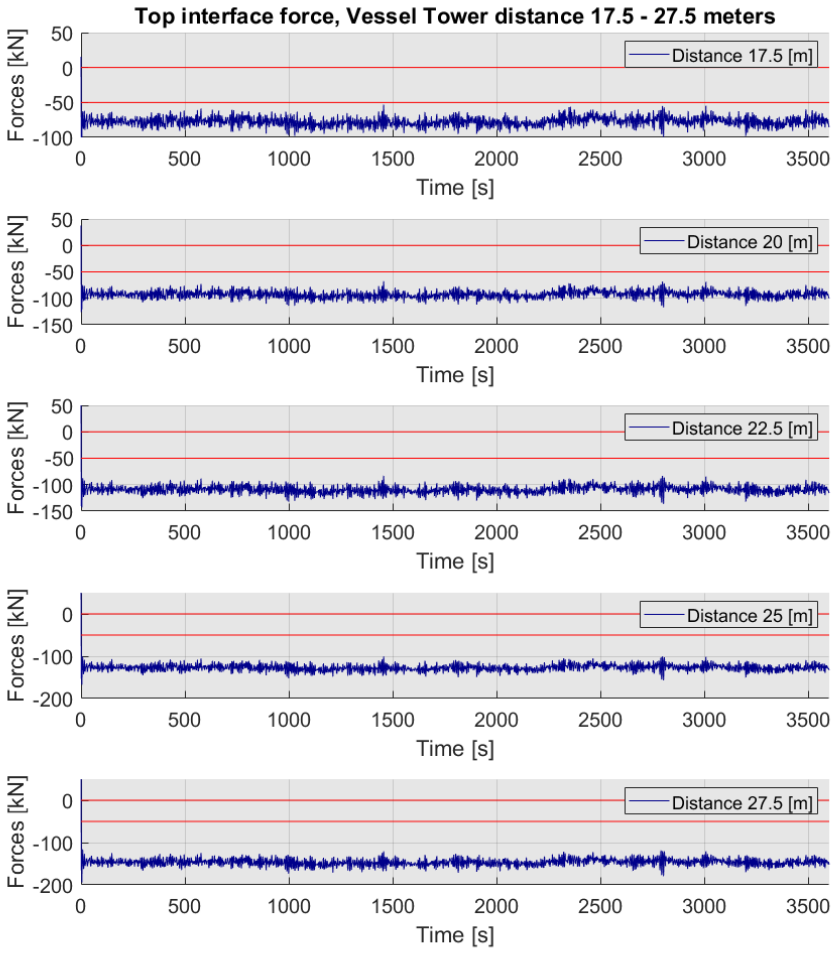

Figure 5.13: Top interface force for vessel and tower distance between 5 and 15 meters

As can be seen in the results, the tower and vessel distance mainly affects the mean of the tower-interface force, with larger distances creating larger forces. The maximum, minimum and mean interface forces for each of the distance are shown in Figure 5.14.

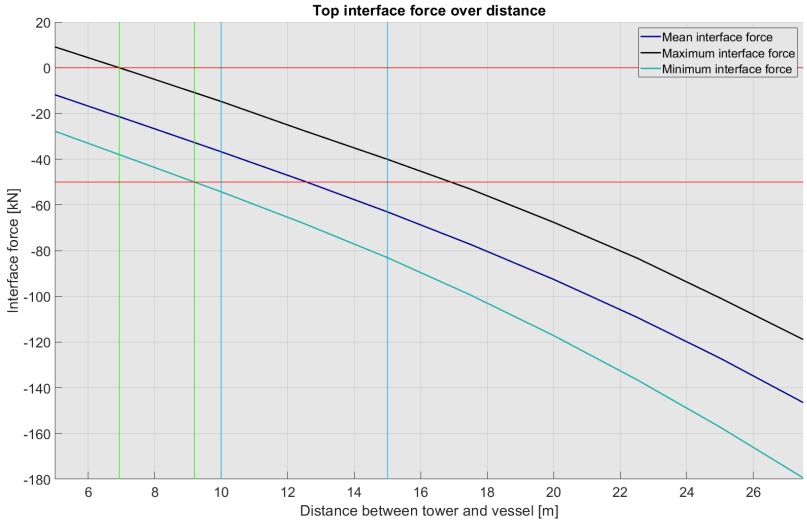

Figure 5.14: Top interface force for vessel and tower distance between 5 and 15 meters

The green lines, between 6.9 meters and 9.2 meters, indicates the range in which the forces remain within the allowable range. This only gives a margin of 2.3 meters. If the vessel will not be able to maintain its position within this small of range if additional environment conditions are considered. This implies that an additional system must be applied to be able to adjust the forcing on the tower, one possibility is the use of winches to reduce the loading.

Considering the trade off between reducing the risk of collision and the forces acting on the tower by the BIT. A distance of between 10 and 15 meters between vessel and tower is preferred. This lies outside the range for which the interface forces remain within the allowable range.

5.3. RELATION BETWEEN THE HS AND THE TOWER DEFLECTION

The last sub-question to be explored is the relation between the Hs and the forces and tower deflections. Simulations were performed for a single load case with the Hs varying between 1 and 10 meters. The top interface force for the Hs up to 5 meters are shown in Figure 5.15.

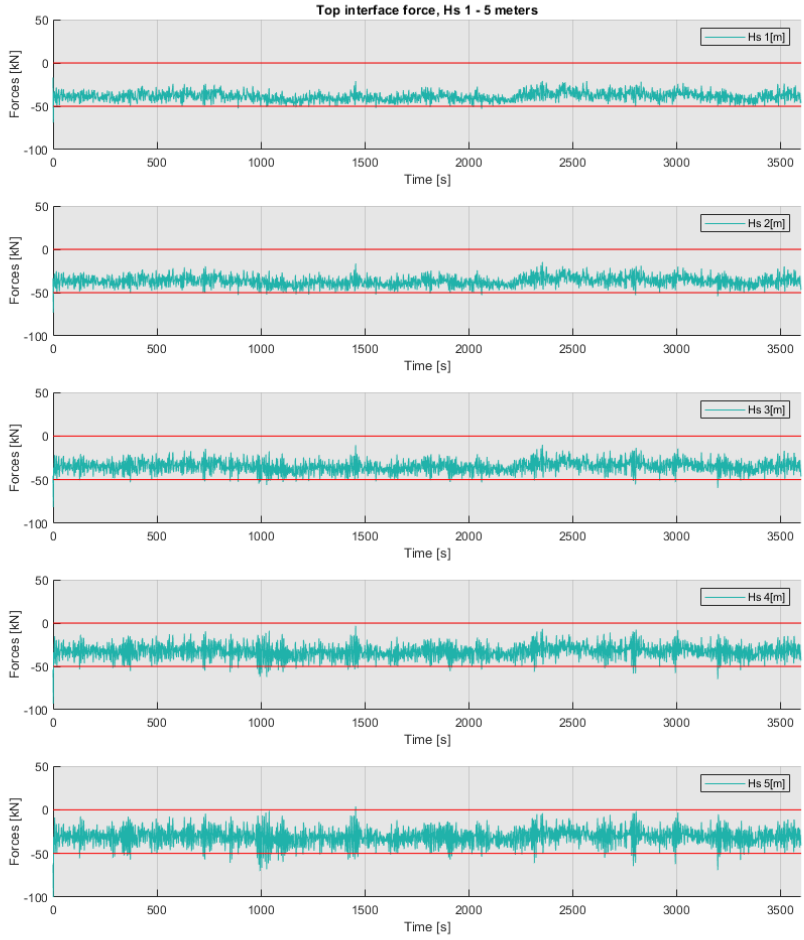

Figure 5.15: Top interface force for Hs between 1 and 5 meters

The resulting maximum deflection of the OWT for each Hs is shown in Table 5.6. The maximum deflection of the tower remains small, even at a sea-state with 10 meter Hs, due to the motion compensation and decoupling system of the BIT. However, it is not realistic for the BIT operate under these conditions, as the model has a perfect motions compensation.

Table 5.6: Maximum tower deflection, Lifting phase: not lifting, Heading at 0°.

Significant wave height	Maximum tower deflection
l m	0.231 m
2 m	0.231 m
3 m	0.231 m
4 m	0.235 m
5 m	0.239 m
6 m	0.242 m
7 m	0.246 m
8 m	0.249 m
9 m	0.253 m
10 m	0.258 m

6

Conclusions & Recommendations

If I have seen further it is by standing on the shoulders of Giants.

Isaac Newton

This final chapter concludes the thesis with the conclusions & recommendations. After analysing the results from the simulations, a conclusion is drawn for the sub-questions posed in this research. In addition, possible solutions for the issues encountered are presented. And finally recommendations are presented for further research into the topic.

6.1. CONCLUSIONS

Below are the conclusions drawn for the research sub-questions.

Are the interface forces on the tower acceptable in conditions comparable to the operational limits of jack-up vessels?
The BIT, for the cases examined, will not be able to operate in conditions comparable to the operational limits of jack-up vessels. The interface forces of the six lifting phases exceed the allowable force range of 0 and -50 kN. The results for each of the lifting phase are elaborated below.

- Not lifting, Midway boom, Top boom: For these three phases the force amplitudes remains within 50 kN. However, the results show peak forces exceeding the limits due to the mean interface force.
- Blade horizontal at the tower-interface: The moment introduced by the blade requires to be counteracted by the top and bottom interface forces, resulting in additional compression and tension for the bottom and top interface respectively. The consequence is a difference between the mean force of the top and bottom interface exceeding 50 kN.
- Blade at an 45° angle at the tower-interface: The moment acting on the tower-interface is lowered due to the blade angle. However, due to the increase in vertical surface area, additional wind loads will be introduced. The difference between the mean top and bottom interface force still exceeds 50 kN.
- Blade vertically at the tower-interface: In this phase, the moment acting on the tower-interface is negligible. However, the wind load is further increased due to the increase in surface area of the blade. The additional wind forces causes the bottom interface force to fluctuate over the allowable limits.

What is the relation between the vessel-tower distance and the interface forces?
The vessel-tower distance affects the mean of the interface forces. Increase in the distance causes an increase in mean interface forces. The distance range for which the interface forces remain within the allowable limits is between 6.9 and 9.2 meters. This range, however, is only applicable for a specific load case. During the lifting process this range will shift depending on the weight and position of the blade. Furthermore the preferred range for the vessel to operate is between 10 and 15 meters, providing a safety margin before the vessel comes into contact with the tower. This implicates that additional measurement must be implemented adjust the interaction forces.

How much does the significant wave height affect the forces and stresses on the tower?
The deflection of the OWT is not governed by the Hs. With considerable increase in Hs will only impact the deflection of the tower slightly as seen in Table 5.6. The results show increasing peak forces, but due to the duration of these forces, the tower deflection is not affected with any significance. This result is expected because of the motion compensation and decoupling of the tool.

The current design of the BIT will not be able to operate under the chosen design conditions. The interface forces for all load cases exceed the allowable limits of 0 and -50 kN. There are two main issues that causes the interface force to be exceeding the limits. First, the mean forces are too high during most of the lifting phases and second, the moment and forces exerted by the blade on the tower-interface are counteracted by the interface forces, causing it to exceed the allowable limits.
There are several ways to address the high mean interface forces. The straightforward method is by increasing the contact surface area. The stresses, which is the limiting factor, will remain at acceptable ranges, while permitting higher forces. A second method, which is more complex, but also provides more control is to add additional mechanical systems, such as winches and hydraulic cylinders to adjust the BIT during the operations.
The counteracting moment of the interface forces due to the blade requires a more complicated solution. The main cause for the exceedance of the limit is due to gravity and wind forces acting on the blade. A possible solution is to find an optimum angle for the blade at which the moment is sufficient low while the force fluctuation due to the wind are still within allowable limits. If this is insufficient, other options to adjust the forces can be considered such as adding hydraulic actuators to control the moment of the tower-interface or to lower the wind conditions in which the BIT can operate allowing for smaller blade angles.

The BIT design explored in this thesis will not be able to satisfy the requirements to operate at the desired environmental conditions. However, the BIT is still early in its development cycle and it will be subjected to multiple iterations. As the BIT shows a lot of potential economically and technically, it is highly valuable to further the research and design of the Tool.

6.2. RECOMMENDATION

To conclude the final part of this thesis the following discussion point and recommendations concerning the dynamic analysis of the BIT are elaborated.

- As mentioned in the conclusion, the BIT requires changes in its design to be able to satisfy the requirements. A natural next step is to design the BIT such that the interface forces remain within the limits. This can be done using the example solutions presented in the conclusion.
- The most critical recommendation for continuation of this research is to validate the numerical model. The dynamic model created in this research only provides an initial insight of the dynamic behaviour of the system. To fully assess the results of the numerical model, a scaled model testing is required to validate the results from the numerical model and further increase the understanding of the dynamic behaviour.
- The governing plane of motion, the vertical plane in the longitudinal direction of the vessel, is investigated. This is chosen based on the assumption that the transversal motions remains small compared to the length of the tower. Thus resulting in only small forces. However, during the development process the design of the BIT changed and this assumption may not be valid. To guarantee the technical viability this plane of motions should be investigated as well.
- The vessel motion considered is determined via the first order wave forces and the RAO of a specific vessel. Further, forces exerted by the BIT are assumed to be negligible compared to the hydrodynamic forces and therefore inconsequential for the vessel motion. Further in-depth research can be performed to determine the consequences of interaction between BIT and different vessel types.
- Investigate different station keeping options, such as mooring lines, dynamic positioning or a combination, and their effects. It is important to determine whether the station keeping has enough capability to keep the vessel within the allowable range. Implementing station keeping allows for the inclusion of additional environmental effects such as the 2nd order wave drift forces, current forces, and wind forces. Unlike the first order wave forces, these environmental forces causes the vessel to drift from the original position and therefore can not be assessed without the implementation of station keeping.
- Wind is assumed to be flowing in only the horizontal direction and the related forces are calculated using coefficients. In reality wind behave in a more complex and chaotic manner. Lift and vortexes induced motions introduces forces and motions not included in this research. This is especially important, due to the involvement of rotor blades, they are designed to interact with wind. This means that they are also strongly affected by changes in the wind.

- The final recommendation is to investigate different types of foundation. One of the reason to choose for a floating solution is to be able to service OWT at deep water depths. These OWT will not be supported by monopiles due to its limitations. Each support structure type has different characteristics and consequently have different interactions. To ensure the BIT is technically viable for these cases it is important to investigate different types of foundation.

REFERENCES

1. **T. Remy, A. Mbistrova**, *Offshore wind in Europe - Key trends and statistics 2017*, WindEurope (February 2018).

2. **D. Fraile, A. Mbistrova**, *Wind in power 2017 - Annual combined onshore and offshore wind energy statistics*, WindEurope (February 2018).

3. **A. Nghiem, I. Pineda**, *Wind energy In Europe: Scenarios for 2030*, WindEurope (September 2017).

4. **LEANWIND consortium**, *Driving Cost Reductions in Offshore Wind*, (November 2017).

5. **M. Florian, J. D. Sørenson**, *Risk-based planning of operation and maintenance for offshore wind farms*, Journal of Marine Science and Engineering (October 2013).

6. **Y. Dalgic, I. Lazakis, O. Turan**, *Vessel charter rate estimation for offshore wind O & M activities*, Department of Naval architecture and marine engineering (September 2015).

7. **J. Cook, et al**, *Consensus on consensus: a synthesis of consensus estimates on human-caused global warming*, Environmental Research Letters Vol. 11 No. 4 (April 2016).

8. **Fisat**, *Safety and Working Guidelines for Rope Access*, (May 2015).

9. **K. de Groot**, *A Novel Method for Installing Offshore Wind Turbine Blades with a Floating Vessel*, marine and transport technology (October 2015).

10. **Saipem**, *Saipem 7000 semi-submersible brochure*, Saipem (June 2018).

11. **D.J. Rixen**, *Engineering Dynamics*, (April 2006)

12. **M.H. Keegan, D.H. Nash, M.M. Stack**, *On erosion issues associated with the leading edge of wind turbine blades*, Journal of Physics D: Applied Physics, (August 2013)

13. **K. Branner, A. Ghadirian**, *Database about blade faults*, DTU Wind Energy E; No. 0067, (Decemeber 2014)

14. **Y. Dalgic et al.**, *Investigation of optimum jack-up vessel chartering strategy for offshore wind farm O & M activities*, Ocean Engineering, (December 2014)

15. **NREL**, *Report on wind turbine subsystem reliability - A Survey of various data bases*, National Renewable energy laboratory (June 2013)

16. **A. Abrous et al.**, *Modeling and Simulation of a Wind Model Using a Spectal Representation Method*, 3rd International Renewable and Sustainable Energy Conference, (December 2015)

17. **E. Branlard**, *Generation of time series from a spectrum*, Wind energy, (February 2010)

18. **Det norske veritas**, *Environmental conditions and environmental loads*, recommended practice (October 2010)

19. **Germanischer Lloyd**, *Structural Design - Rules and standards*, GL IV-6-4, (December 2007)

20. **H.E. Hinnant**, *Derivation of a Tapered p-Version Beam Finite Element*, NASA Technical paper 2931 (August 1989)

21. **J. van der Tempel**, *Design of support structures for offshore wind turbines*, (April 2006)

22. **L.H. Holthuijsen**, *Waves in oceanic and coastal waters*, (February 2010)

23. **J.M.J. Journée, W.W. Massie**, *Offshore hydromechanics*, (January 2001)

24. **R.Q. van der Linde, A.L. Schwab**, *Multibody Dynamics B*, (February 2010)

25. **D. Gross, W. Hauger, J. Schröder, W.A. Wall, S. Govindjee**, *Engineering Mechanics 3*, (2011)

A

RESULTS TIME DOMAIN SIMULATION

This appendix shows the simulation in the time domain under difference load cases.

A

A.1. LIFTING SEQUENCE: NOT LIFTING

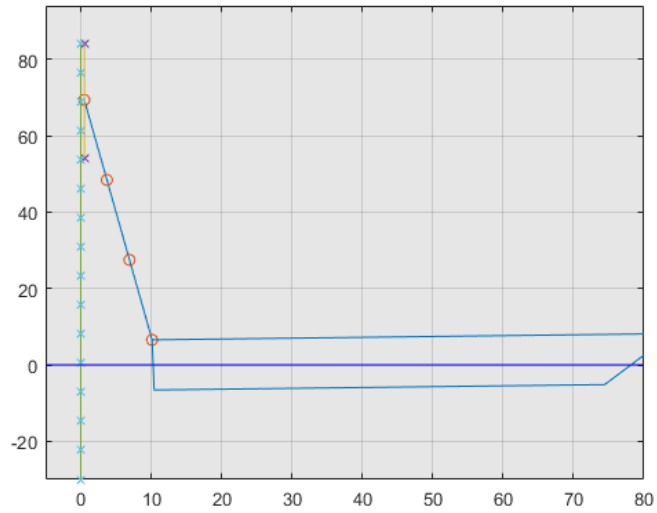

Figure A.1: Lifting sequence: not lifting

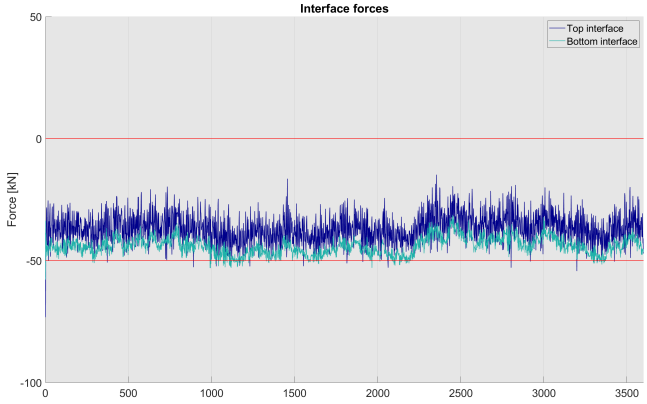

Figure A.2: Simulation parameters: Hs 2 meters, Heading 0°, not lifting

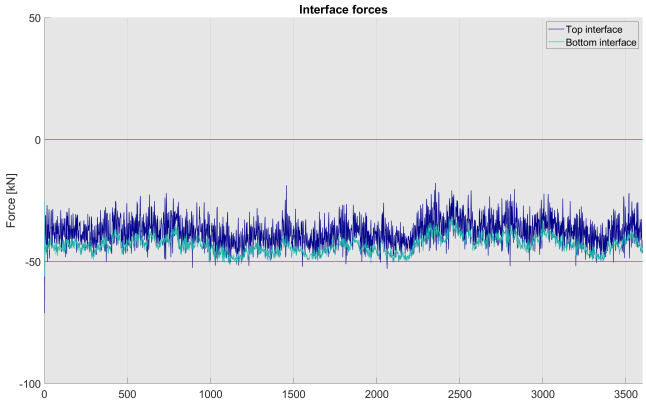

Figure A.3: Simulation parameters: Hs 1.5 meters, Heading 0°, not lifting

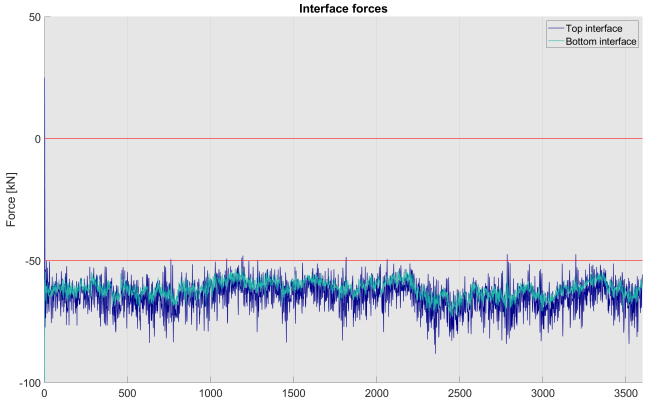

Figure A.4: Simulation parameters: Hs 2 meters, Heading 180°, not lifting

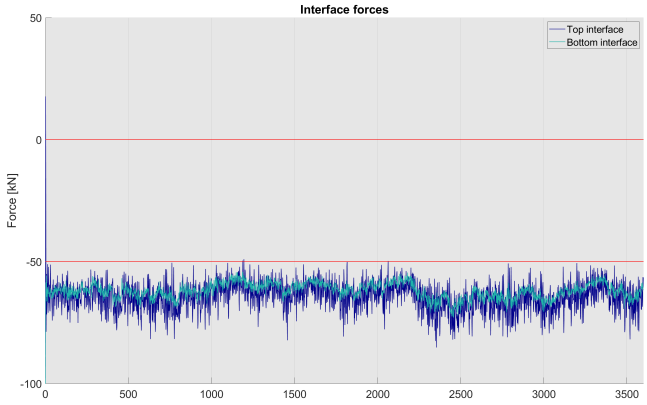

Figure A.5: Simulation parameters: Hs 1.5 meters, Heading 180°, not lifting

A.2. LIFTING SEQUENCE: MIDWAY BOOM

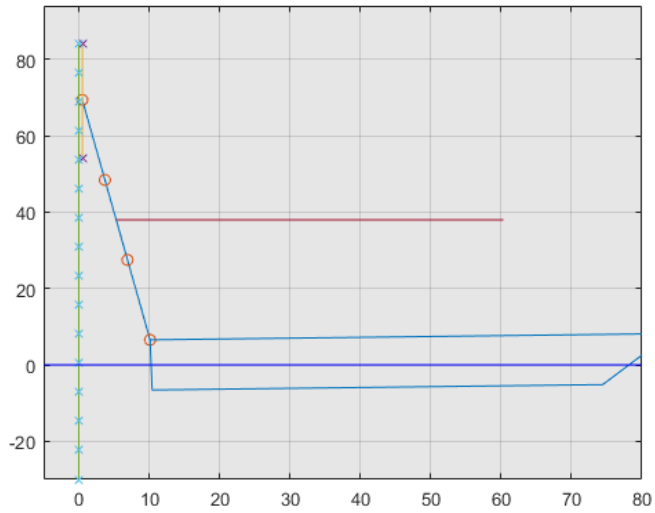

Figure A.6: Lifting sequence: Blade midway boom

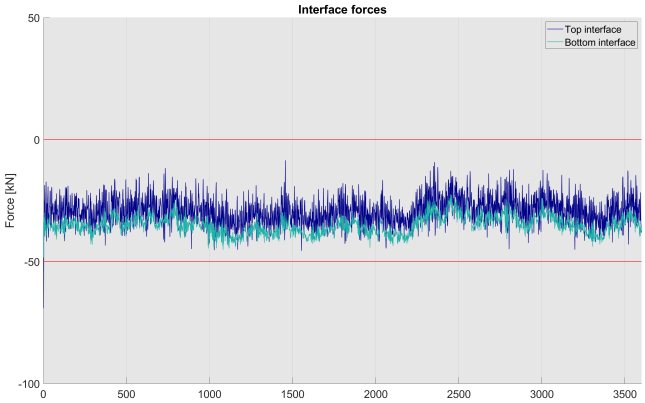

Figure A.7: Simulation parameters: Hs 2 meters, Heading 0°, midway boom

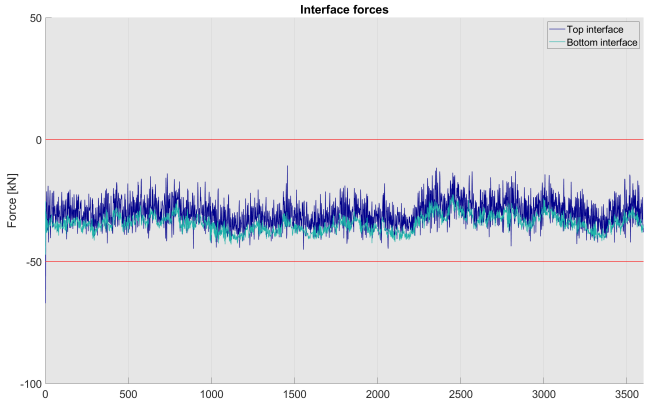

Figure A.8: Simulation parameters: Hs 1.5 meters, Heading 0°, midway boom

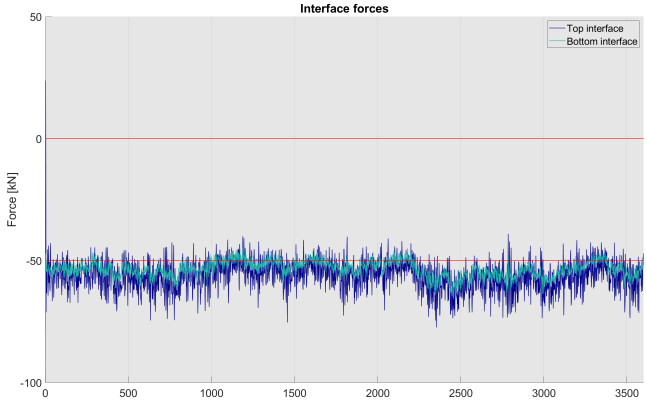

Figure A.9: Simulation parameters: Hs 2 meters, Heading 180°, midway boom

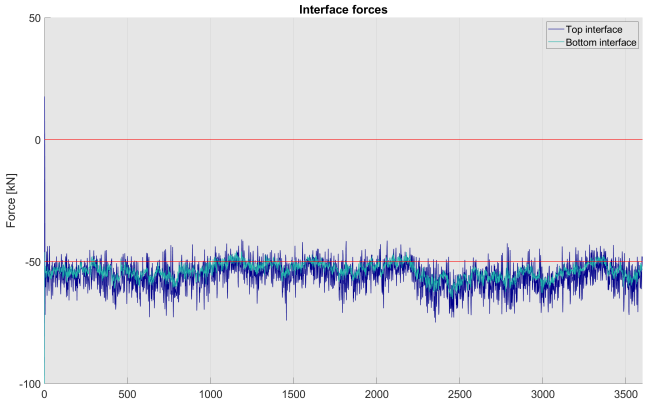

Figure A.10: Simulation parameters: Hs 1.5 meters, Heading 180°, midway boom

A

A.3. LIFTING SEQUENCE: BLADE AT THE TOP OF THE BOOM

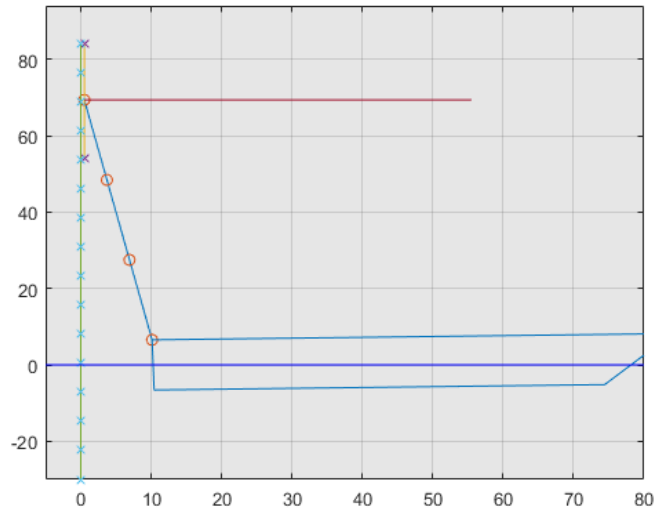

Figure A.11: Lifting sequence: Blade at the top of the boom

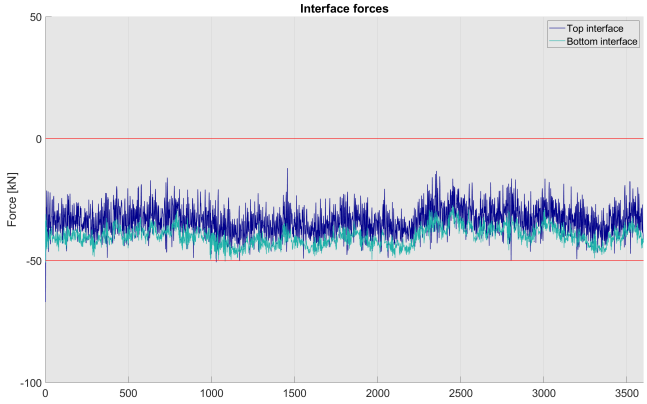

Figure A.12: Simulation parameters: Hs 2 meters, Heading 0°, top of the boom

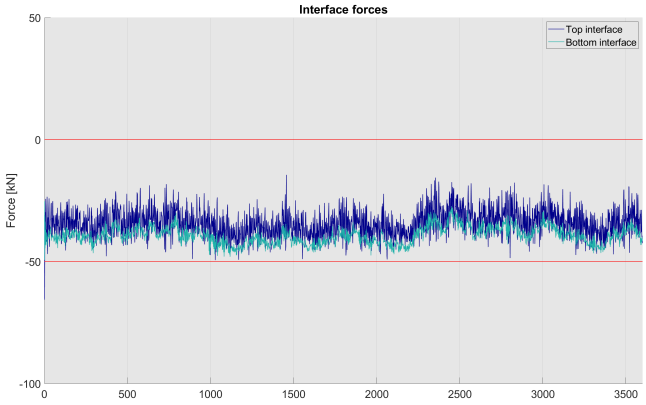

Figure A.13: Simulation parameters: Hs 1.5 meters, Heading 0°, top of the boom

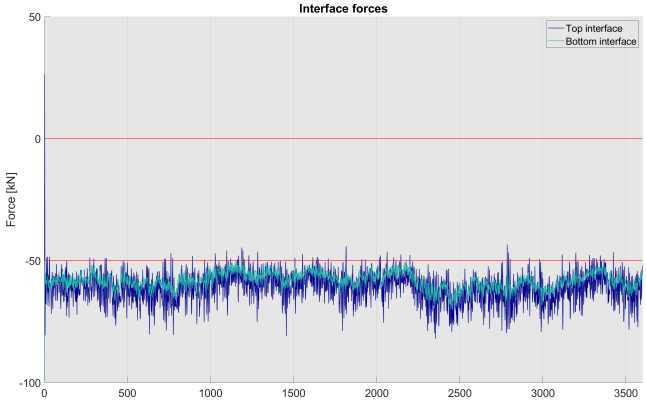

Figure A.14: Simulation parameters: Hs 2 meters, Heading 180°, top of the boom

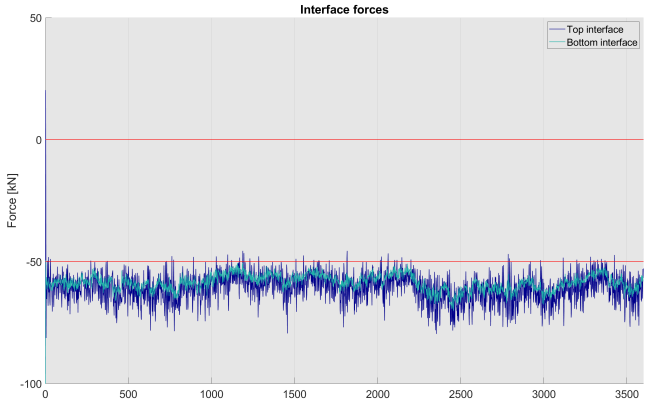

Figure A.15: Simulation parameters: Hs 1.5 meters, Heading 180°, top of the boom

A.4. LIFTING SEQUENCE: BLADE AT THE TOWER INTERFACE

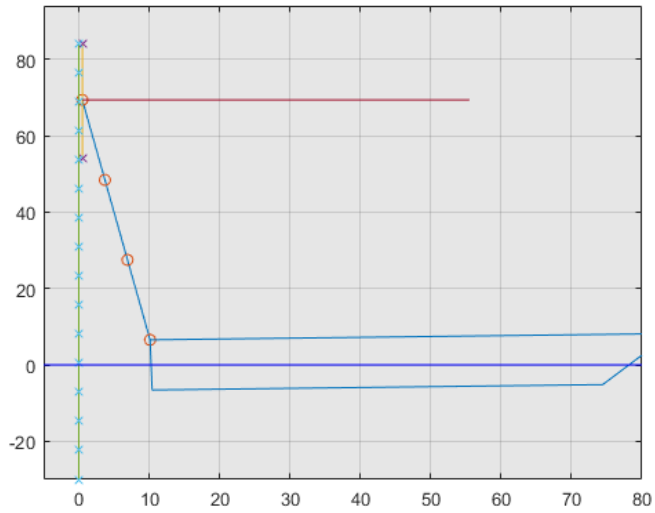

Figure A.16: Lifting sequence: Blade horizontal at the tower interface

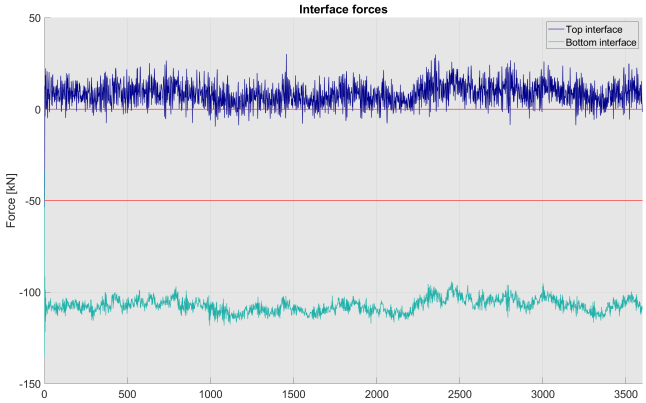

Figure A.17: Simulation parameters: Hs 2 meters, Heading 0°, blade horizontal at the tower interface

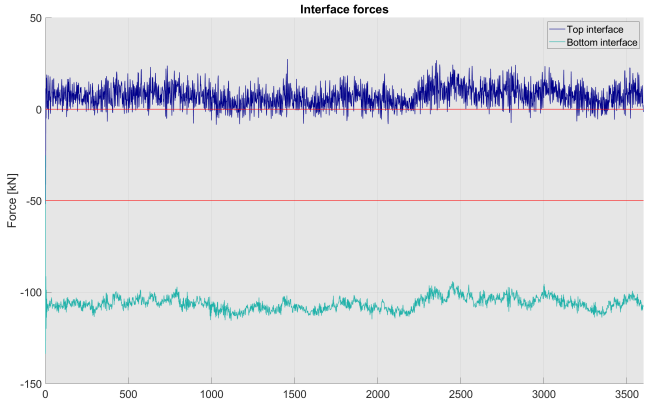

Figure A.18: Simulation parameters: Hs 1.5 meters, Heading 0°, blade horizontal at the tower interface

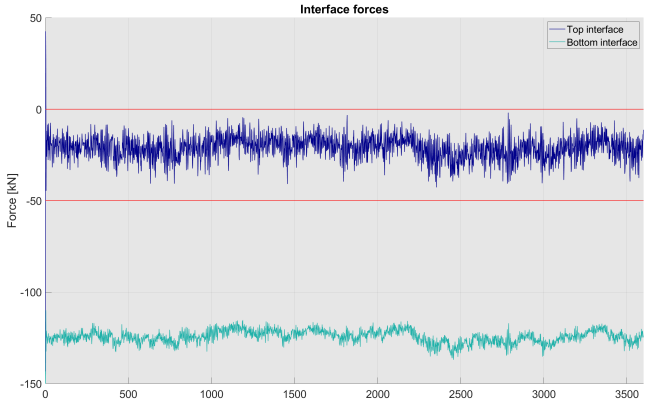

Figure A.19: Simulation parameters: Hs 2 meters, Heading 180°, blade horizontal at the tower interface

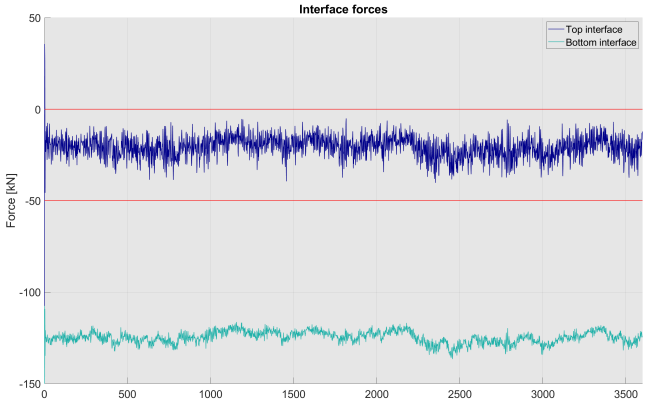

Figure A.20: Simulation parameters: Hs 1.5 meters, Heading 180°, blade horizontal at the tower interface

A

A.5. LIFTING SEQUENCE: BLADE AT THE TOWER INTERFACE UNDER AN ANGLE OF 45°

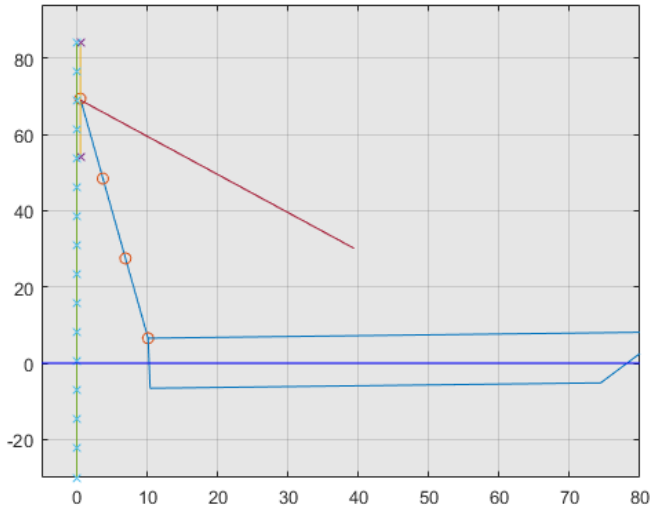

Figure A.21: Lifting sequence: Blade at the tower interface under 45°angle

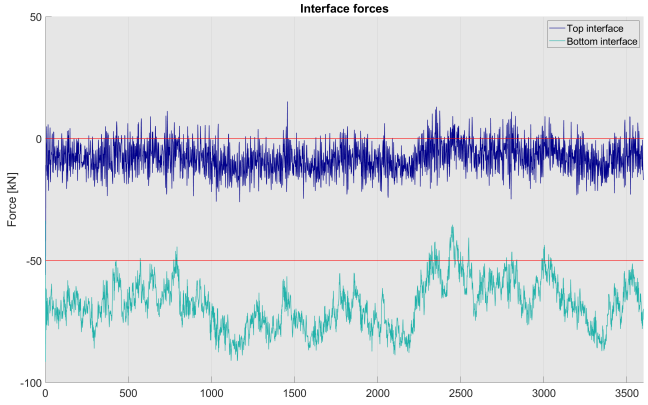

Figure A.22: Simulation parameters: Hs 2 meters, Heading 0°, blade at an 45° angle at the tower interface

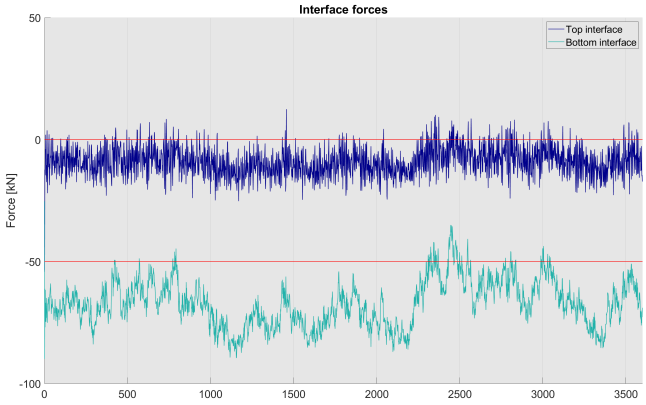

Figure A.23: Simulation parameters: Hs 1.5 meters, Heading 0°, blade at an 45° angle at the tower interface

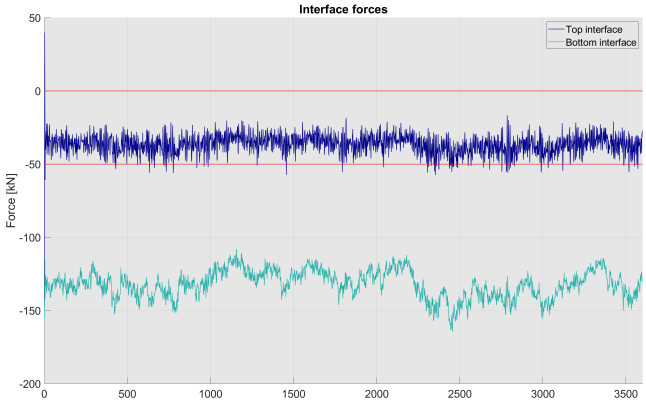

Figure A.24: Simulation parameters: Hs 2 meters, Heading 180°, blade at an 45° angle at the tower interface

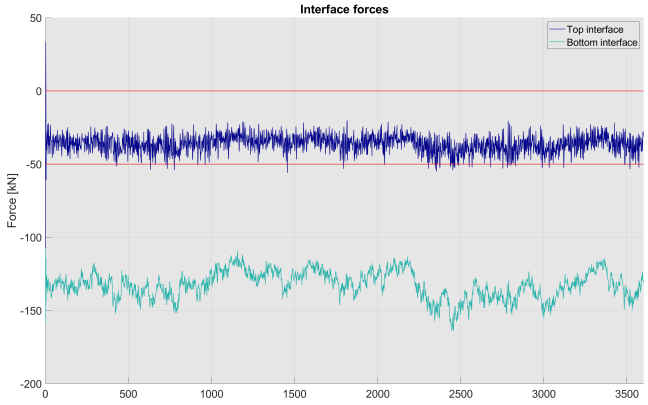

Figure A.25: Simulation parameters: Hs 1.5 meters, Heading 180°, blade at an 45° angle at the tower interface

A.6. LIFTING SEQUENCE: BLADE VERTICALLY AT THE TOWER INTERFACE

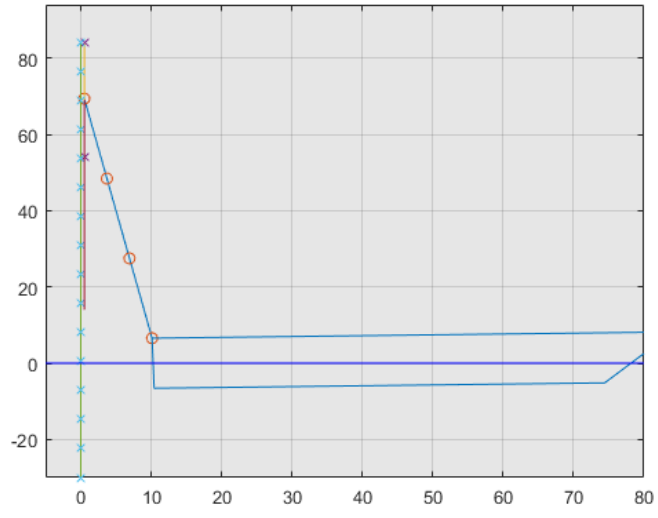

Figure A.26: Lifting sequence: Blade vertically at the tower interface

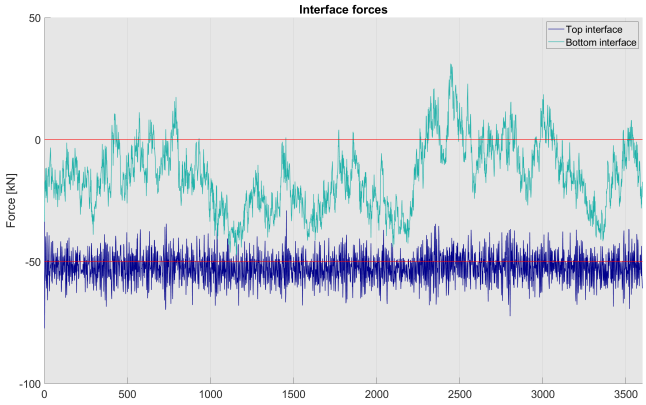

Figure A.27: Simulation parameters: Hs 2 meters, Heading 0°, Blade vertically at the tower interface

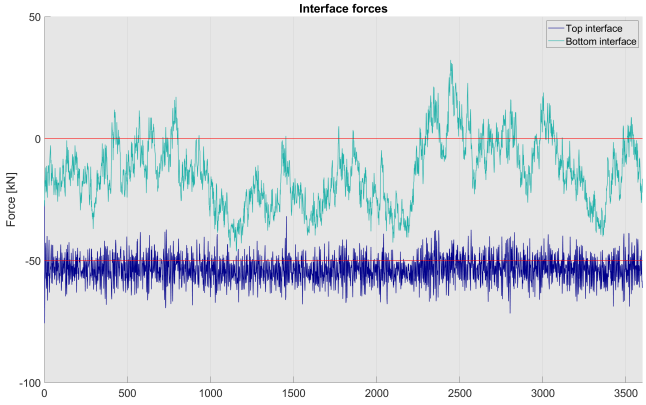

Figure A.28: Simulation parameters: Hs 1.5 meters, Heading 0°, Blade vertically at the tower interface

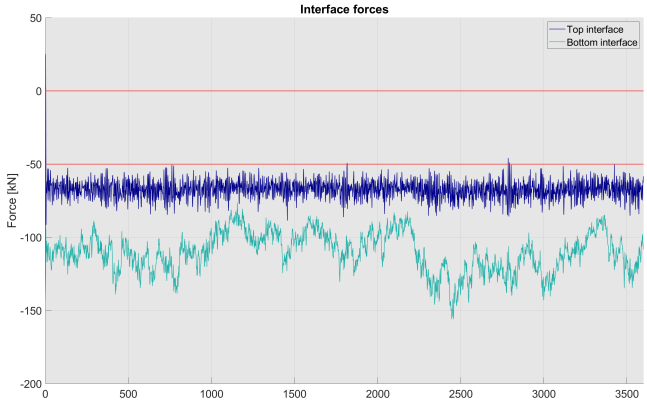

Figure A.29: Simulation parameters: Hs 2 meters, Heading 180°, Blade vertically at the tower interface

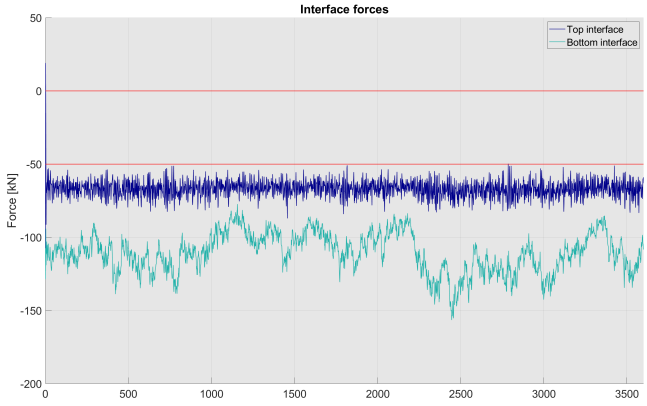

Figure A.30: Simulation parameters: Hs 1.5 meters, Heading 180°, Blade vertically at the tower interface

B

FINITE ELEMENT METHOD

Finite element is a method that allows a continuous system to be approximated numerically, by discretizing the continuous member into smaller elements. The equation of motions is derived for each element and combined to form the EOM of the whole member. The EOM of an element can be derived using the Euler-Lagrange equation.

$$\mathbb{L} = \mathbb{T} - \mathbb{V} = \frac{1}{2}\int_l \int_A \rho V(x,y,z)^2 - \sigma(x,y,z)\epsilon(x,y,z)\, dA\, dx \tag{B.1}$$

Assuming linear stress-strain relation and bending deformation:

$$\begin{aligned} \epsilon &= y\frac{dw}{dx} \\ \sigma &= E\epsilon \end{aligned} \tag{B.2}$$

This makes the potential term:

$$\mathbb{V} = \frac{1}{2}\int_l \int_A E(y\frac{dw}{dx})^2\, dA\, dx \tag{B.3}$$

Combining it with the 2nd moment of area gives:

$$\int_A y^2 dA = I\frac{1}{2}EI\int_l (\frac{dw}{dx})^2\, dx \tag{B.4}$$

The full equation becomes:

$$\mathbb{L} = \mathbb{T} - \mathbb{V} = \frac{\rho A}{2}\int_0^l V^2\, dx - \frac{EI}{2}\int_0^l (\frac{dw}{dx})^2 dx \tag{B.5}$$

This can yet be solved due to the velocity and deflection V and w, these are still unknown. To find the EOM these will be assumed to comply to a shape function. The velocity and deflection over the length of the element will be assumed to have to following form.

$$S = c_1 + c_2 x + c_3 x^2 + C_4 x^4 \tag{B.6}$$

The unknown constants can be found by substituting in the boundary conditions. The boundary conditions are:

$$\text{At } x = 0: \quad S = w_1, \quad \frac{dS}{dx} = \theta_1$$

$$\text{At } x = l: \quad S = w_2, \quad \frac{dS}{dx} = \theta_2$$

Solving for the unknown constants gives:

$$\begin{aligned} C_1 &= w_1 \\ C_2 &= \theta 1 \\ C_3 &= \frac{-3w_1 - 2l\theta_1 + 3w_2 - l\theta_2}{l^2} \\ C_4 &= \frac{2w_1 - l\theta_1 - 2w_2 - l\theta_2}{l^3} \end{aligned} \tag{B.7}$$

The shape functions, considering the constants, becomes as follows:

$$S = \left(1 - \frac{3x^2}{l^2} + \frac{2x^3}{l^3}\right) w_1 + \left(x - \frac{2x^2}{l} + \frac{x^3}{l^2}\right) \theta_1 + \left(\frac{3x^2}{l^2} - \frac{2x^3}{l^3}\right) w_2 + \left(\frac{-x^2}{l} + \frac{x^3}{l^2}\right) \theta_2 \tag{B.8}$$

This shape function is used to assume the displacement and velocity of the start and end note. The EOM can now be derived using the Lagragian formulation.

$$\sum_{i=1}^{4} \frac{d}{dt} \frac{\partial \mathbb{L}}{\partial V_i} - \frac{\partial \mathbb{L}}{\partial w_i} = 0 \tag{B.9}$$

This gives the following set of equations

$$\frac{\rho A l}{420} \begin{bmatrix} 156 & 22l & 54 & -13l \\ 22l & 4l^2 & 13l & -3l^2 \\ 54 & 13l & 156 & -22l \\ -13l & -3l^2 & -22l & 4l^2 \end{bmatrix} \begin{bmatrix} \ddot{w}_1 \\ \ddot{\theta}_1 \\ \ddot{w}_2 \\ \ddot{\theta}_2 \end{bmatrix} - \frac{EI}{L^3} \begin{bmatrix} 12 & 6l & -12 & 6l \\ 6l & 4l^2 & -6l & 2l^2 \\ -12 & -6l & 12 & -6l \\ 6l & 2l^2 & -6l & 4l^2 \end{bmatrix} \begin{bmatrix} w_1 \\ \theta_1 \\ w_2 \\ \theta_2 \end{bmatrix} \tag{B.10}$$

To get the EOM for the whole system, all the mass and stiffness amtrixes need to be combined. This is done by the following manner.

$$\begin{bmatrix} A_{11} & A_{12} & A_{13} & A_{14} & & \\ A_{21} & A_{22} & A_{23} & A_{24} & & \\ A_{31} & A_{32} & A_{33} + B_{11} & A_{34} + B_{12} & B_{13} & B_{14} \\ A_{41} & A_{42} & A_{43} + B_{21} & A_{44} + B_{22} & B_{23} & A_{24} \\ & & B_{31} & B_{32} & B_{33} & B_{34} \\ & & B_{41} & B_{42} & B_{43} & B_{44} \end{bmatrix} \tag{B.11}$$

This is done because the 3rd and 4th DOF of the first element is the same nod as the 1st and 2nd DOF of the second element. By increasing the number of element, the results will get increasingly accurate.